TABLE OF CONTENTS

NASA Contractor Report 3183

A Compressible Solution of the Navier-Stokes Equations for Turbulent Flow About an Airfoil

S. J. Shamroth and H. J. Gibeling

CONTRACT NAS1-15214
OCTOBER 1979

NASA

NASA Contractor Report 3183

A Compressible Solution of the Navier-Stokes Equations for Turbulent Flow About an Airfoil

S. J. Shamroth and H. J. Gibeling
Scientific Research Associates, Inc.
Glastonbury, Connecticut

Prepared for
Langley Research Center
under Contract NAS1-15214

National Aeronautics
and Space Administration

**Scientific and Technical
Information Branch**

1979

BLANK PAGE

TABLE OF CONTENTS

SUMMARY

A compressible time-dependent solution of the Navier-Stokes equations including a transition-turbulence model is obtained for the isolated airfoil flow field problem. The equations are solved by a consistently split linearized block implicit scheme due to Briley and McDonald. A nonorthogonal body fitted coordinate system is used which has maximum resolution near the airfoil surface and in the region of the airfoil leading edge. The transition-turbulence model is based upon the turbulence kinetic energy equation and predicts regions of laminar, transitional and turbulent flow. Mean flow field and turbulence field results are presented for an NACA 0012 airfoil at zero and nonzero incidence angles at Reynolds number up to one million and low subsonic Mach numbers.

INTRODUCTION

Flow over an isolated airfoil, particularly in the presence of separation, is a problem which clearly demonstrates the importance of developing efficient and accurate numerical solutions for the Navier-Stokes equations. The isolated airfoil problem arises in a variety of practical applications including the aircraft wing, control surfaces, propellers and helicopter rotor blades. When these components are at small or modest incidence, accurate flow field predictions can be obtained by combining inviscid and boundary layer analyses in a noniterative mode (Refs. 1 and 2). If the boundary layer-inviscid flow interaction remains localized, accurate flow field predictions can be obtained even with small regions of separated flow present (Ref. 3). However, if significant regions of separation are present, then the usual boundary layer assumption that the pressure distribution about the airfoil is either independent of the viscous flow development near the surface or can be approximated by a simple inviscid displacement surface, becomes significantly in error and a full Navier-Stokes solution which simultaneously predicts the pressure and velocity fields is required if valid predictions are to be obtained.

Turning to the helicopter problem in particular, a phenomenon of primary interest is that of dynamic stall. Static stall occurs when an airfoil is placed at large incidence in a steady stream; dynamic stall occurs when the incidence is a function of time. Dynamic stall differs from its static counterpart in two major ways. First of all, the maximum lift obtainable under dynamic conditions is greater than that under static conditions. Secondly, though under static conditions lift is uniquely related to incidence, under dynamic conditions stall depends upon the time history of motion and has a hysteresis loop associated with it. As the helicopter blade travels through the rotor disc, the blade experiences a varying incidence angle. Over most of the disc the blade will be unstalled (i.e., the flow will not contain any large separated regions leading to a decrease in blade lift or a generation of large blade moment coefficients); however, over a portion of the disc large regions of separated flow may appear and over these regions the blade performance will deteriorate. This time history dependence of the problem makes dynamic stall prediction a particularly difficult task.

Despite its complex nature dynamic stall has been the subject of a number of theoretical and experimental investigations over the past years. The behavior of the leading edge separation bubble has been investigated by both Velkhoff, Blaser and Jones (Ref. 4) and Isogai (Ref. 5) and the dynamic stall mechanism itself has been scrutinized by McCroskey and Phillipe (Ref. 6), McCroskey, Carr and McAlister (Ref. 7) and Parker (Ref. 8). More recent investigations have been reported at the AGARD Symposium on Unsteady Aerodynamics (Ref. 9). These include the unsteady flow investigation of Saxena, Fejer and Morkovin (Ref. 10) and the dynamic stall review paper of Philippe (Ref. 11).

In addition to the large number of experimental investigations, a variety of analytical approaches have focused upon the dynamic stall problem. A review of these methods has been given by McCroskey in Ref. 12. Among these approaches are inviscid vortex shedding models of Ham and Garelick (Ref. 13) and Bandu, Sanger and Souquet (Ref. 14), the data correlation approach of Carta and his coworkers (e.g., Ref. 15) and the semi-empirical models of Ericsson and Reding (Ref. 16) and Lang (Ref. 17). These were followed by the approaches of Crimi and Reeves (Ref. 18), Shamroth and Kreskovsky (Ref. 2) and Kreskovsky, Shamroth and Briley (Ref. 1), all of which are based upon solutions of fluid dynamic equations. More recently, motivated by a desire to relieve some of the restrictive assumptions and/or empiricism of earlier methods, attention has focused upon Navier-Stokes solutions to the isolated airfoil problem. In an early work of this type, Mehta and Lavan (Ref. 19) solved a stream function vorticity formulation of the laminar incompressible Navier-Stokes equations to predict flow about an impulsively started airfoil. Although this method required considerable computer run time, its excellent results convincingly demonstrated the practical benefits which could be realized from Navier-Stokes solutions. In a recent work Mehta (Ref. 20) used a more efficient numerical procedure to solve incompressible laminar flow about an airfoil oscillating through incidence regimes in which stall occurs. Another Navier-Stokes analysis is that of Wu and Sampath (Ref. 21) and Wu, Sampath and Sankar (Ref. 22) who have applied the Wu-Thompson integro-differential formulation (Ref. 23) to the impulsively started airfoil problem. In a similar vein Kinney and Cielak (Refs. 24 and 25) have applied a vorticity formulation of the Navier-Stokes equations to the incompressible airfoil flow field problem and Hodge and Stone (Ref. 26) have investigated stalled airfoils again using a Navier-Stokes solution.

Although arguments can be made in favor of one of these procedures versus the other, it is clear that as a group these efforts have demonstrated that application of Navier-Stokes formulations to the airfoil problem is both feasible and practical. However, these procedures all have had three major limitations associated with them: (i) incompressibility, (ii) laminar flow and (iii) lack of generality of airfoil geometry. In regard to the first of these items, the preceding analyses all are incompressible and none can be extended readily to the compressible case. In regard to the second limitation, all these analyses assume the flow to be laminar although presumably this assumption can be relieved in a straightforward manner if simple eddy viscosity and forced transition concepts are accepted. Insofar as geometry is concerned it is noted that coordinate systems for the Navier-Stokes solutions are at least one degree more stringent in the coordinate system smoothness than those required for inviscid analyses, and hence a straightforward extension of an existing coordinate system developed for solution of the inviscid equations may not be possible. The Navier-Stokes analyses mentioned above have used a coordinate system which either is conformal or is generated from a solution of Poisson's equation. The conformal requirement is a very stringent one which could make it very expensive or even impossible to investigate many airfoil shapes of practical interest by virtue of the resulting coordinates having numerous and rapid changes in curvature. The requirement that the coordinate system be generated from a solution of Poisson's equation is not nearly as constraining as is the requirement that it be conformal. In principal most if not all airfoils of interest could be generated in this manner. However, as discussed by Thompson, Thames and Mastin (Ref. 27), in practice convergence problems can arise when obtaining a solution to the Poisson equation required to generate the coordinate grid. In addition practical difficulties can arise in specifying a coordinate grid having high resolution in regions where the greatest need for resolution exists; i.e., in regions in which the dependent variables change rapidly. As a result of these restrictions, a more general coordinate generation system would be a distinct advantage in applying Navier-Stokes analyses to the airfoil flow field.

The problem of eliminating the incompressible assumption from the full Navier-Stokes equations for airfoil flow field calculations has been overcome by Verhoff (Ref. 28), Deiwert (Ref. 29), Levy (Ref. 30) and Gibeling, Shamroth

and Eiseman (Ref. 31). Verhoff applied MacCormack's fully explicit method (Ref. 32) to the airfoil problem; however, since the procedure is fully explicit, a small time step is necessary to maintain numerical stability as a result of the locally refined mesh in the boundary layer and long computer run times result. In this regard conditionally stable schemes such as fully explicit schemes are not an optimum choice when mesh refinement is required for boundary layer definition; in these schemes the allowable marching step size is limited by the spatial step size leading to large run times. On the other hand, unconditionally (in a linear sense) stable schemes such as some of the implicit schemes do not suffer from this characteristic. Both Deiwert's (Ref. 29 and Levy's (Ref. 30) analyses are based upon MacCormack's more recent hybrid implicit-explicit-characteristics scheme (Ref. 33). By virtue of an enlarged stability bound this new procedure is much more efficient than the original MacCormack procedure (Ref. 32) for airfoil calculations; however, it does present formidable coding problems.

Another approach to the airfoil problem has been taken by Steger (Refs. 34 and 35) who has used an approximate viscous analysis in conjunction with the coordinate generation procedure of Thompson, Thames and Mastin (Ref. 36) to predict laminar flow about an airfoil. The equations solved by Steger (Refs. 34 and 35) are not the full Navier-Stokes equations but rather a reduced set of equations which retain only those viscous terms important in thin shear flows. As a consequence Steger's approach could be invalid when the shear layer no longer remained thin or even became significantly inclined to the coordinate along which the thin shear layer approximation is made. Both of these problems could be particularly significant in the stall problem under consideration here. The numerical scheme used by Steger is that given by Beam and Warming (Ref. 37), who used the time linearization approach of Briley and McDonald (Ref. 38) in conjunction with the approximate factorization technique of D'Yakonov (see Yanenko, Ref. 39) to produce a linearized block implicit scheme. More recently Briley and McDonald (Ref. 40) have shown that the Beam and Warming (Ref. 37) derivation produces essentially the same consistently split linearized block implicit scheme as that developed earlier by Briley and McDonald (Ref. 38) using the Douglas-Gunn ADI procedure (Ref. 41) in its natural extension to systems of partial differential equations. Gibeling, Shamroth and Eiseman (Ref. 31) applied this Briley-McDonald procedure to solve

the Navier-Stokes equations for the flow about a cylinder and an airfoil, although in this study, as in Refs. 28, 34, and 35, the calculations were performed for laminar flow.

The present effort extends the compressible flow work of Gibeling, Shamroth and Eiseman (Ref. 31) and concentrates upon the latter two of the previously mentioned problem areas: (ii) turbulent flow and (iii) coordinate generality. The procedure adds a turbulence model to the airfoil flow field and demonstrates the practicality of constructive nonorthogonal coordinate systems by producing calculations about an NACA 0012 airfoil using a constructive coordinate system.

LIST OF SYMBOLS

Except where dimensions are specified, all quantities in the following are nondimensional; physical velocities are normalized by u_r, density by ρ_r, pressure by $\rho_r u_r^2$, dynamic viscosity by μ_r, and time by (L/u_r) where L is the reference length.

a_o - Turbulence constant

a_1 - Turbulence structural coefficient

A - Coefficient in pressure-velocity law

B - Coefficient in pressure-velocity law

C - Airfoil chord

C_1 - Turbulence structural coefficient

C_2 - Turbulence structural coefficient

C_μ - Turbulence structural coefficient

$D^{\epsilon}_{\alpha\gamma}$ - Coefficient in tensor form of momentum equation

$E^{\epsilon}_{\alpha\gamma}$ - Coefficient in tensor form of momentum equation

$F^{\beta}_{ij\alpha}$ - Coefficient in tensor form of momentum equation

F - Vector in Navier-Stokes equations

F_1 - Vector in Navier-Stokes equations

g_{ij} - Metric tensor coefficient

g^{ij} - Inverse metric coefficient

G - Vector in Navier-Stokes equations

G_1 - Vector in Navier-Stokes equations

$G_{\alpha ij}$ - Coefficient in tensor form of momentum equation

LIST OF SYMBOLS (CONT'D)

$I_{\alpha\nu}$ - Coefficient in tensor form of momentum equation

J - Jacobian

k - Turbulence kinetic energy

ℓ - Turbulence length scale

$L^{\omega}_{\alpha\nu}$ - Coefficient in tensor form of momentum equation

L_r - Reference length, taken as airfoil chord

$M_{\alpha\nu}$ - Coefficient in tensor form of momentum equation

P - Pressure

Q_{ν}^{β} - Coefficient in tensor form of momentum equation

Re - Reynolds number

R_{α} - Coefficient in tensor form of momentum equation

R_T - Turbulence Reynolds number

S_{α} - Coefficient in tensor form of momentum equation

t - Time

u - Cartesian velocity

u_r - Reference velocity, usually taken as free stream velocity at upstream infinity

v - Cartesian velocity

v^i - Contravariant velocity component

w - Vector in Navier-Stokes equation

x - Cartesian coordinate parallel to chord

y - Cartesian coordinate normal to chord

y_s - Distance normal from surface

y^α - General coordinate

δ - Boundary layer thickness

δ^α_β, $\delta_{\alpha\beta}$ - Kronecker delta

ε - Turbulence energy dissipation

η - General coordinate

κ - Von-Karman Constant

μ - Viscosity

μ_r - Reference viscosity, taken as free stream viscosity at upstream infinity

μ_T - Turbulent viscosity

ξ - General coordinate

ρ - Density

ρ_r - Reference density, taken as free stream density at upstream infinity

σ_κ - Prandtl number for turbulence energy transfer

σ_ε - Prandtl number for turbulence dissipation transfer

τ - Shear stress

ANALYSIS

The Governing Equations

The Mean Flow Equations

The flow field about an airfoil is governed by the Navier-Stokes equations and in conjunction with a suitable turbulence model a solution of the time-dependent form of these equations would serve to predict the flow field for both laminar and turbulent flows. The form of the equations expressed in the more common coordinate systems can be found in standard fluid dynamic texts (e.g., Ref. 42 and 43) and the equations themselves have been derived in general tensor form by McVitte (Ref. 44) for inviscid flow and by Walkden (Ref. 45) for viscous flow.

When solving the Navier-Stokes equations for flow about airfoils, basic decisions must be made concerning the coordinate system to be used and the form of equations to be solved. The presence of flow field bounding surfaces which do not fall on coordinate lines presents significant difficulties in applying boundary conditions and unacceptably large truncation errors could result. One method of eliminating this problem transforms the governing equations from the usual Cartesian coordinates to a new coordinate system having the airfoil surface as a coordinate line; in general, the process may lead to a nonorthogonal coordinate system.

Several candidate forms of the governing equations present themselves for solution in the general nonorthogonal case. For example, Gibeling, Shamroth and Eiseman (Ref. 31) have solved the set of Navier-Stokes equations in general tensor form using the density and the contravariant components of the velocity vector as dependent variables. The governing momentum conservation equations were the components of the vector equations aligned in the coordinate directions. The equations were written in the form

Continuity Equation

$$\frac{\partial}{\partial t}(\rho J) + \frac{\partial}{\partial y^{\beta}}(\rho v^{\beta} J) = 0 \qquad (1)$$

Momentum Equation

$$\frac{\partial}{\partial t}\left(J\, g_{\alpha i}\, \rho v^i\right) + K\frac{\partial \rho}{\partial y^\alpha} + F^{\beta}_{ij\alpha}\frac{\partial}{\partial y^\beta}\left(\rho v^i v^j\right) + L^{\omega}_{\alpha\nu}\frac{\partial v^\nu}{\partial y^\omega}$$

$$+ D^{\epsilon}_{\alpha\gamma}\frac{\partial^2 {}_v\gamma}{\partial y^\beta \partial y^\epsilon} + R_\alpha \rho + I_{\alpha\nu} v^\nu + M_{\alpha\beta}\, \rho v^\beta + G_{\alpha ij}\, \rho v^i v^j = S_\alpha \qquad (2)$$

where t is time, J is the Jacobian, $g_{\alpha\beta}$ is a metric tensor coefficient, v^i is a contravariant component of velocity in the i^{th} coordinate direction, ρ is density, y^i is a coordinate and

$$K = AJ$$

$$F^{\beta}_{ij\alpha} = \left(g_{\alpha i}\,\delta^{\beta}_{j} + B g_{ij}\,\delta^{\beta}_{\alpha}\right) J \qquad (3)$$

$$G_{\alpha ij} = \frac{\partial F^{\beta}_{ij\alpha}}{\partial y^\beta} - \frac{J}{2}\frac{\partial g_{\epsilon\beta}}{\partial y^\alpha}\left(\delta_i{}^{\epsilon}\,\delta^{\beta}_{j} + B g_{ij}\, g^{\epsilon\beta}\right)$$

$$M_{\alpha\beta} = -J\frac{\partial g_{o\beta}}{\partial y^\alpha}$$

$$R_\alpha = A\frac{\partial J}{\partial y^\beta}\,\delta^{\beta}_{\alpha} - \frac{J}{2}\left[\frac{\partial g_{oo}}{\partial y^\alpha} + A\frac{\partial g_{\epsilon\beta}}{\partial y^\alpha}\, g^{\epsilon\beta}\right]$$

$$D^{\beta\epsilon}_{\alpha\gamma} = \frac{\mu}{Re} J\left[\frac{2}{3}\,\delta^{\beta}_{\alpha}\,\delta^{\epsilon}_{\gamma} - g_{\alpha\gamma}\, g^{\epsilon\beta} - Q^{\beta}_{\gamma}\,\delta^{\epsilon}_{\alpha}\right]$$

$$S_\alpha = \frac{\mu}{Re}\frac{\partial g_{\epsilon\beta}}{\partial y^\alpha}\left[\frac{1}{3}\, g^{\epsilon\beta}\frac{\partial J}{\partial t} - \frac{J}{2}\, g^{\omega\epsilon}\, g^{\gamma\beta}\frac{\partial g_{\gamma\omega}}{\partial t}\right]$$

$$- \frac{2}{3}\frac{\partial}{\partial y^\alpha}\left(\frac{\mu}{Re}\frac{\partial J}{\partial t}\right) + \frac{\partial}{\partial y^\beta}\left(\frac{\mu}{Re} J\, g^{\epsilon\beta}\frac{\partial g_{\alpha\epsilon}}{\partial t}\right)$$

$$I_{\alpha\nu} = \frac{\partial E^\beta_{\alpha\nu}}{\partial y^\beta} + \frac{\frac{\mu}{Re}}{2}\frac{\partial g_{\epsilon\beta}}{\partial y^\alpha}\left[J\, g^{\omega\epsilon}\, g^{\gamma\beta}\frac{\partial g_{\gamma\omega}}{\partial y^\nu} - \frac{2}{3}\frac{\partial J}{\partial y^\nu}\, g^{\epsilon\beta}\right]$$

$$L^\omega_{\alpha\nu} = E^\omega_{\alpha\nu} + \frac{\partial D_{\alpha\nu}{}^{\beta\omega}}{\partial y^\beta} + \frac{\frac{\mu}{Re} J}{2}\frac{\partial g_{\epsilon\beta}}{\partial y^\alpha}\left[g^{\omega\epsilon}\, Q^\beta_\nu + g^{\omega\beta}\, Q_\nu{}^\epsilon - \frac{2}{3}\, g^{\epsilon\beta}\,\delta_\nu{}^\omega\right]$$

where

$$Q^\beta_\gamma = \delta^\beta_\gamma - g_{\gamma o}\, g^{o\beta}$$

$$E^\beta_{\alpha\gamma} = \frac{\mu}{Re}\left[\frac{2}{3}\frac{\partial J}{\partial y^\gamma}\,\delta_\beta{}^\alpha - J\, g^{\epsilon\beta}\frac{\partial g_{\alpha\epsilon}}{\partial y^\alpha}\right] \qquad (4)$$

and A and B relate pressure, velocity and density through the gas law equation which is written for constant total temperature as

$$P = \rho\left[A + B g_{ij} v^i v^j\right] \qquad (5)$$

In the previous equations $g^{\alpha\beta}$ are coefficients of the inverse metric tensor, μ is viscosity, Re is Reynolds number, Latin indices are summed from 1 to 3 and Greek indices are summed from 0 to 3; v^0 is defined as unity. In addition all quantities have been made nondimensional; physical velocities have been normalized by a reference velocity, u_r, density by a reference density, ρ_r, pressure by $\rho_r u_r^2$, dynamic viscosity by μ_r and time by L/u_r where L is a reference length. This represents the first candidate form of the equations.

Solution of the equations in this form yielded excellent results for flow about a circular cylinder (Ref. 31), however, resolution difficulties resulting from large truncation error were encountered when the contravariant velocity components were used as dependent variables for flow about an airfoil. Therefore, the authors of Ref. 31 solved the airfoil flow field by employing the physical velocity components in the coordinate direction as dependent variables rather than the contravariant components of the velocity vector. This was accomplished by noting that in an orthogonal coordinate system the physical velocity component u_i could be expressed in terms of metric data and the contravariant velocity components v^i as

$$u_i = v^i \Big/ \sqrt{g_{ii}} \tag{6}$$

where no summation on the repeated index is implied. Therefore v^i was replaced in the governing equations by $(v^i / \sqrt{g_{ii}})\ \sqrt{g_{ii}}$ and the equations solved for $u_i = v^i / \sqrt{g_{ii}}$. When this approach was used, a solution for flow about a Joukowski airfoil was obtained without difficulty, and although Eq. (6) is restricted to orthogonal coordinates a more general expression of this type could be used for nonorthogonal coordinates. This approach represents the second candidate form.

The third candidate form solves a divergence form of the Navier-Stokes equations in which the Cartesian velocity components are the dependent variables. The governing equations (for constant total temperature flow) are continuity and the momenta equations in the two coordinate directions; however, the independent spatial variables are transformed from the Cartesian coordinates x,y to a new set of coordinates ξ,η where

$$\xi = \xi(x,y,t)$$

$$\eta = \eta(x,y,t)$$

$$\tau = t \tag{7}$$

As shown by Steger (Refs. 34 and 35) the governing equations then become

$$\frac{\partial W/D}{\partial \tau} + \frac{\partial}{\partial \xi}\left[\frac{W\xi_t}{D} + \frac{F\xi_x}{D} + \frac{G\xi_y}{D}\right] + \frac{\partial}{\partial \eta}\left[\frac{W\eta_t}{D} + \frac{F\eta_x}{D} + \frac{G\eta_y}{D}\right]$$
$$= \frac{1}{Re}\left[\frac{\partial}{\partial \xi}\left(\frac{F_1\xi_x}{D} + \frac{G_1\xi_y}{D}\right) + \frac{\partial}{\partial \eta}\left(\frac{F_1\eta_x}{D} + \frac{G_1\eta_y}{D}\right)\right] \tag{8}$$

where

$$D = \xi_x\eta_y - \xi_y\eta_x$$

$$W = \begin{pmatrix} \rho \\ \rho u \\ \rho v \end{pmatrix}, \quad F = \begin{pmatrix} \rho u \\ \rho u^2 + p \\ \rho uv \end{pmatrix}, \quad G = \begin{pmatrix} \rho v \\ \rho uv \\ \rho v^2 + p \end{pmatrix} \quad F_1 = \begin{pmatrix} 0 \\ \tau_{xx} \\ \tau_{xy} \end{pmatrix} \quad G_1 = \begin{pmatrix} 0 \\ \tau_{xy} \\ \tau_{yy} \end{pmatrix} \tag{9}$$

Steger used these equations in conjunction with a thin shear layer stress approximation to predict an airfoil flow field (Refs. 34 and 35) and this approach was carefully considered as a candidate approach in the present investigation, although of course modifying the approach so as to retain the full stress tensor appropriate to the Navier-Stokes equations.

The final candidate form considered in the present investigation also is based upon density and the Cartesian velocities as dependent variables and continuity and the momenta equations written in the Cartesian directions as governing equations. However, in this approach the equations are not solved in divergence form but rather are solved in the quasi-linear form

$$\frac{\partial W}{\partial \tau} + \xi_t\frac{\partial W}{\partial \xi} + \xi_x\frac{\partial F}{\partial \xi} + \xi_y\frac{\partial G}{\partial \xi} + \eta_t\frac{\partial W}{\partial \eta} + \eta_x\frac{\partial F}{\partial \eta} + \eta_y\frac{\partial G}{\partial \eta}$$
$$= \frac{1}{Re}\left[\xi_x\frac{\partial F_1}{\partial \xi} + \eta_x\frac{\partial F_1}{\partial \eta} + \xi_y\frac{\partial G_1}{\partial \xi} + \eta_y\frac{\partial G_1}{\partial \eta}\right] \tag{10}$$

In deciding upon an approach to use in the present effort, the first candidate form was eliminated from consideration because of the resolution difficulties it exhibited in the airfoil calculation of Ref. 31. An examination of the expressions for $I_{\alpha\nu}$ and $E^{\beta}_{\alpha\nu}$ in Eq. (3) shows that the second candidate form requires second derivatives of metric coefficients which in turn requires third derivatives of y^{α} with respect to the Cartesian coordinates x and y. In contrast the third and fourth candidate approaches only require evaluations of second derivatives of y^{α} with respect to the Cartesian coordinates. This requirement of one less degree of differentiability upon the grid coordinate transformation represents a distinct advantage for the third and fourth candidates, since a less smooth coordinate system is required and can be more easily generated. For this reason the second approach was eliminated from further consideration. Thus the final choice was narrowed to these latter two possible approaches.

Before proceeding to airfoil calculations, both the third and fourth procedures were used to repeat the cylinder flow field calculation previously presented in Ref. 31. The results of this calculation are shown in Fig. 1. The calculations were run until the maximum change in each dependent variable during one body traverse time divided by the dependent variable itself dropped to below one per cent. As can be seen in Fig. 1, the results of the fourth candidate approach, Eq. (10), were in good agreement with the three sets of results presented in Ref. 31. In contrast the results of the third candidate approach showed considerable disagreement with all other results.

A careful examination of the equations was performed to determine the reason for the poor predictions obtained from formulation number three. After a term by term examination of the equations, the major difficulty was found to reside in the momenta equation pressure gradient terms. In this formulation the pressure term is of the form $\partial Gp/\partial\xi$ where G is a function of the geometric data. The numerical representation of this term is

$$\frac{\partial Gp}{\partial \xi} \doteq \frac{G(\xi+\Delta\xi)p(\xi+\Delta\xi) - G(\xi-\Delta\xi)p(\xi-\Delta\xi)}{2\Delta\xi} \tag{11}$$

In the cylinder calculations, p varies from grid point to grid point in the fourth significant figure whereas G varies in the first or second significant figure. As a result pressure changes were commensurate with the geometric data truncation error, an obviously undesirable situation.

Although the cylinder represents only one case, the resulting poor treatment of the pressure gradient term by the third formulation is still expected to be a problem in performing airfoil calculations. The problem would be somewhat alleviated with increasing Mach number since increasing Mach number is accompanied by increasing pressure difference from point to point. In addition, the cylinder geometry represents a relatively stringent test of formulation three. The airfoil is a much more streamlined body than the cylinder with the coordinate curvature being much less pronounced over most of the flow field. Nevertheless, large coordinate curvature does occur in the airfoil leading edge region. Therefore even if the problems exhibited by the strong conservation approach are not as serious in the airfoil case as they proved to be in the cylinder case, they are still expected to be present. A more detailed discussion of the problem is given by Shamroth and Gibeling in Ref. 46.

Based upon these considerations, the fourth coordinate formulation was chosen for the present effort.

The Turbulence Model

Since the present effort addresses the problem of turbulent flow, it is necessary to specify a turbulence model suitable for this problem. One complicating factor in hypothesizing and applying a turbulence model for the isolated airfoil flow field is that the flow is not turbulent everywhere. Far from the airfoil the flow is laminar. In addition, even near the airfoil surface the flow is laminar in the vicinity of the airfoil leading edge. Thus any proposed model must be capable of dealing with laminar, transitional and turbulent flow. The turbulent flow problem including laminar and transitional regions has been treated approximately but quite successfully for the simpler problem of boundary layer flows by McDonald and Fish (Ref. 47), Shamroth and McDonald (Ref. 48) and Kreskovsky, Shamroth and McDonald (Ref. 49). These investigators applied an integral form of the turbulence kinetic energy equation in conjunction with the

boundary layer mean flow momentum equations to predict a wide variety of flows in both forward and reverse transition. As shown in Refs. 47-49, the model gives excellent agreement between prediction and data for a variety of typical test cases. In an alternative but similar approach Jones and Launder (Ref. 50) and Launder and Jones (Ref. 51) used a two-equation turbulence model in predicting relaminarizing flows, but did not apply this model to the forward transition problem. Application of the model to the forward transition process in boundary layers was initiated by Pridden (Ref. 52) who obtained predictions of transitional boundary layers (see Launder and Spalding (Ref. 53)). Later the Launder-Jones model was applied to the forward transition problem again in boundary layers by Quemard and Michel (Ref. 54); however, none of the calculations presented in Ref. 54 proceeded successfully through transition. In summary, at the initiation of the present effort, calculations through transition in both the forward and reverse direction had been made routinely for boundary layer flows using an integral form of the turbulence kinetic energy equation (Refs. 47-49); however, questions remained concerning the problem of predicting transitional flows via the differential equation of turbulence kinetic energy for airfoil flow fields.

The approach taken in the present effort assumes an isotropic turbulent viscosity, μ_T, relating the Reynolds' stress tensor to mean flow gradients.

$$-\overline{\rho u_i' u_j'} = \mu_T\left[\left(\frac{\partial u_i}{\partial x_j} + \frac{\partial u_j}{\partial x_i}\right) - \frac{2}{3}\frac{\partial u_k}{\partial x_k}\delta_{ij}\right] \tag{12}$$

Using Favre averaging (Ref. 55) the governing equations then are identical to the laminar equations with velocity and density being taken as mean variables and viscosity being taken as the sum of the molecular viscosity, μ, and the turbulent viscosity, μ_T. Originally, it was intended that the turbulent viscosity be obtained from the two-equation turbulence model in which the turbulence kinetic energy, k, and turbulence dissipation rate, ε, were taken as dependent variables. This model has been used by several investigators (e.g., Refs. 50 and 51) for fully turbulent flow fields and, in fact, has been utilized successfully by Gibeling, McDonald and Briley (Ref. 56) in a study of turbulent combusting flows made using a reacting flow version of the same numerical procedure applied in the present investigation.

The equations governing the development of k and ϵ have been given by several authors (e.g., Launder and Spalding (Ref. 53)) and in Cartesian coordinates are given as

$$\frac{\partial \rho k}{\partial t} + \frac{\partial \rho u k}{\partial x} + \frac{\partial \rho v k}{\partial y} = \frac{\partial}{\partial x_k}\left[\left(\mu + \frac{\mu_T}{\sigma_k}\right)\frac{\partial k}{\partial x_k}\right] + \mu_T\left(\frac{\partial u_i}{\partial x_k} + \frac{\partial u_k}{\partial x_i}\right)\frac{\partial u_i}{\partial x_k} - \rho\epsilon - 2\mu\frac{\partial k^{1/2}}{\partial x_j}\frac{\partial k^{1/2}}{\partial x_j} \tag{13a}$$

$$\frac{\partial \rho \epsilon}{\partial t} + \frac{\partial \rho u \epsilon}{\partial x} + \frac{\partial \rho v \epsilon}{\partial y} = \frac{\partial}{\partial x_j}\left[\left(\mu + \frac{\mu_T}{\sigma_\epsilon}\right)\frac{\partial \epsilon}{\partial x_j}\right] + C_1\frac{\epsilon}{k}\mu_T\left(\frac{\partial u_i}{\partial x_k} + \frac{\partial u_k}{\partial x_i}\right)\frac{\partial u_i}{\partial x_k} - C_2\frac{\epsilon^2\rho}{k} - 2\mu\mu_T\left[\left(\frac{\partial^2 u_i}{\partial x_k \partial x_l}\right)\right]^2 \tag{13b}$$

In Eqs. (13a) and (13b) σ_k and σ_ϵ are Prandtl numbers for k and ϵ respectively and C_1 and C_2 are empirical functions. The equations are discussed in some detail in Ref. 53 and this discussion will not be repeated here. The turbulent viscosity is related to k and ϵ via the Prandtl-Kolmogorof constitutive equation

$$\mu_T = \rho C_\mu k^2/\epsilon \tag{14}$$

In the present analysis the following values were assumed

$$\sigma_\epsilon = 1.3$$

$$\sigma_k = 1.0$$

$$C_1 = 1.55 \tag{15}$$

For fully developed turbulent flow $C_\mu = .09$ and $C_2 = 2.$; in relaminarizing flows Jones and Launder (Ref. 50) give

$$C_\mu = 0.09 \exp\left[-2.5(1. + R_T/50.)\right]$$

$$C_2 = 2.0\left\{1.0 - 0.3\left[\exp(-R_T^2)\right]\right\} \tag{16}$$

however, although this expression has given good results in relaminarizing flows, it has not led to the successful prediction of flows undergoing forward transition in Ref. 54. Therefore, it was felt if a transition model were to be obtained, Eq. (16) should be modified and the successful integral turbulence energy procedure of (Refs. 47-49) was used for guidance. This procedure utilizes a turbulence function a_1 where

$$a_1 = C_\mu^{1/2}/2 \tag{17}$$

and a_1 is taken as a function of a turbulence Reynolds number of the form

$$a_1 = a_0\left[\frac{f(R_T)}{100}\right] \Bigg/ \left\{1.0 + 6.66\, a_0\left[\frac{f(R_T)}{100} - 1\right]\right\} \tag{18}$$

where

$$a_0 = .0115$$

$$f(R_T) = 100.\, R_T^{0.22} \qquad R_T \le 1$$

$$f(R_T) = 68.1\, R_T + 614.3 \qquad R_T \ge 40 \tag{19}$$

and a cubic curve was fit for values of R_T between 1 and 40. As previously discussed, Ref. 47-49 utilized an integral form of the turbulence kinetic energy and therefore R_T was defined as an average value.

$$R_T = \frac{1}{\delta}\int_0^{\delta} \nu_T dy \Big/ \frac{1}{\delta}\int_0^{\delta_s} \nu dy_s \tag{20}$$

In the present effort R_T was defined as the local ratio of turbulent to laminar viscosity, a_1 was evaluated via Eq. (18), C_μ related to a_1 via Eq. (17) and C_2 was evaluated via Eq. (16).

In the early stages of the present effort the mean flow Navier-Stokes equations were solved in conjunction with the partial differential equations governing turbulence kinetic energy and turbulence dissipation equations given earlier; however, problems arose with the solution. The problem areas were those regions in which the flow was expected to be laminar or transitional rather than fully turbulent. Regions of this type are found far from the airfoil and in the vicinity of the airfoil leading edge. One problem which arose concerned evaluation of turbulent viscosity via Eq. (14). In regions where k is small, μ_T should be small; however, in terms of the model μ_T depends on the ratio of k^2/ε and therefore regions of small k can exist simultaneously with regions of large μ_T if the predicted value of ε is small enough. Since regions of small turbulence kinetic energy should coincide with regions of small turbulent viscosity by definition, such behavior is unacceptable.

The problem of ensuring small turbulent viscosities far from the airfoil regardless of the values of k and ε was solved by modifying the viscosity law so that

$$\mu_T = \rho C_\mu \left(1 - e^{-(y_s-\delta)/\delta}\right)\frac{k^2}{\varepsilon} \tag{21}$$

for $y_s > \delta$

The use of Eq. (21) ensured small turbulent viscosities far from the airfoil. The second problem, the region near the airfoil leading edge, proved much more troublesome. In this region the calculation led to negative values of k and/or ϵ and then became unstable. It is possible that this behavior either represents a flaw in the model for laminar and transitional flow or is related to starting the solution from an unrealistic initial k-ϵ profile. The physical source of the problem has not yet been determined, although the numerical problems clearly reside in a stiffness of the governing partial differential equation (McDonald, Ref. 57). Because of the difficulties encountered, the two-equation model was not pursued further in this effort but rather a model combining the turbulence kinetic energy equation with a specified length scale was used.

In this model the length scale was taken as a minimum value of two lengths; a wall length and a wake length. The wall length was assumed to be given by a conventional wall damped Prandtl's mixing length, viz

$$\ell = \kappa y_s \left(1 - e^{-y_s^+/27}\right) \tag{22}$$

with a maximum value of 0.09 δ. In Eq. (22) κ is the von Karman constant taken as 0.43, y_s^+ is the dimensionless distance from the airfoil surface and δ is the boundary layer thickness. The wake length scale was taken as $\ell = .05\delta$ where δ is the wake thickness. Rather than update the boundary layer wake thickness at each time step, for the present the analysis assumed the boundary layer thickness over the first ten per cent chord region to be given by

$$\delta = k_1 x^{1/2} + k_2 \tag{23}$$

and over the last eighty percent chord to be given by

$$\delta = k_3 x^{0.8} \tag{24}$$

where k_1, k_2 and k_3 were chosen at convenient program restart time steps to fit

the generated velocity solution. The two δ formulations were smoothly joined in a blending region, $0.10 \leq x/c \leq 0.20$. Although a step-by-step update of δ based upon the calculated velocity or shear stress field would be preferable, in the interim the present approach assures a smooth variation of δ with distance along the chord and is considered acceptable for the present demonstration. It is anticipated that in subsequent work the local value of the boundary layer thickness will be used and the present strategy was used simply to avoid possible numerical problems arising from the determination and use of a time instantaneous boundary layer thickness.

When applying the turbulence kinetic energy equation with a specified length scale, the turbulent viscosity appearing in the turbulence kinetic energy source term, $\mu_T(\partial u_i/\partial x_k + \partial u_k/\partial x_i)\partial u_i/\partial x_k$, is replaced by Eq. (21) and the dissipation rate ϵ is expressed in terms of k and ℓ by

$$\epsilon = C_\mu^{3/4} \frac{k^{3/2}}{\ell} \tag{25}$$

The resulting equation then is solved to predict the turbulence kinetic energy field.

The Numerical Procedure

The numerical procedure used to solve the governing equation is a consistently split linearized block implicit scheme originally developed by Briley and McDonald (Ref. 39) and embodied in a computer code termed MINT, an acronym for Multi-dimensional Implicit Nonlinear Time-dependent. The basic algorithm was further developed and applied to both laminar and turbulent duct flows by Briley, McDonald and Gibeling (Ref. 58). Subsequently, a three-dimensional compressible Navier-Stokes combustor flow analysis employing the MINT procedure was developed by Gibeling, McDonald and Briley (Ref. 56) and this procedure was then employed by Levy, Shamroth, Gibeling and McDonald (Ref. 59) to determine the feasibility for computing a turbulent shock-wave boundary layer interaction with an implicit method. More recently Gibeling, Shamroth and Eiseman (Ref. 31) have applied the Briley-McDonald scheme to flow about a cylinder and an isolated airfoil. Since the scheme has been outlined

in detail in several publications available in the open literature, it will not be detailed here. Rather only a brief outline of the procedure will be given with more detail in the Appendix; the reader interested in further detail is referred to Refs. 31, 38 and 58).

The method can be outlined as follows: the governing equations are replaced by an implicit time difference approximation, optionally a backward difference or Crank-Nicolson scheme. Terms involving nonlinearities at the implicit time level are linearized by Taylor expansion about the solution at the known time level, and spatial difference approximations are introduced. The result is a system of multidimensional coupled (but linear) difference equations for the dependent variables at the unknown or implicit time level. To solve these difference equations, the Douglas-Gunn (Ref. 41) procedure for generating alternating-direction implicit (ADI) schemes as perturbations of fundamental implicit difference schemes is introduced in its natural extension to systems of partial differential equations. This technique leads to systems of coupled linear difference equations having narrow block-banded matrix structures which can be solved efficiently by standard block-elimination methods.

The method centers around the use of a formal linearization technique adapted for the integration of initial-value problems. The linearization technique, which requires an implicit solution procedure, permits the solution of coupled nonlinear equations in one space dimension (to the requisite degree of accuracy) by a one-step noniterative scheme. Since no iteration is required to compute the solution for a single time step, and since only moderate effort is required for solution of the implicit difference equations, the method is computationally efficient; this efficiency is retained for multidimensional problems by using ADI techniques. The method is also economical in terms of computer storage, in its present form requiring only two time-levels of storage for each dependent variable. Furthermore, the ADI technique reduces multi-dimensional problems to sequences of calculations which are one-dimensional in the sense that easily-solved narrow block-banded matrices associated with one-dimensional rows of grid points are produced. Consequently, only these one-dimensional problems require rapid-access storage at any given stage of the solution procedure, and the remaining flow variables can be saved on auxiliary storage devices if desired.

The Coordinate System

The choice and construction of a coordinate system is an important component in the successful solution of the isolated airfoil problem. The presence of bounding surfaces in a flow field which do not fall upon coordinate lines present significant difficulties for numerical techniques which solve the Navier-Stokes equations. If a bounding surface (such as the airfoil surface) does not fall upon a coordinate line, undue numerical errors may arise in the application of boundary conditions and considerable effort may be required to reduce these errors to an acceptable level. Although this problem arises in both viscous and inviscid flows, it is more severe in viscous flows where no-slip conditions on solid walls can combine with boundary condition truncation error to produce numerical solutions which are both qualitatively and quantitatively in error. Thus coordinate systems are sought in which each no-slip surface of the specific problem falls on a coordinate line.

In addition to requiring that no-slip surfaces fall on coordinate lines, other considerations constrain the choice of a suitable coordinate system. The two most important of these are smoothness of the coordinate system and distribution of grid points. Since the governing equations (e.g., see Eq. (10) of the present report) contain derivatives of the transformation, any transformation chosen must have a degree of smoothness and continuity which allows accurate representation of these derivatives. Secondly, in viscous flow problems different regions have different characteristic length scales and thus fine grid resolution must be available in some regions of the flow field whereas only relatively coarse resolution need be maintained in other regions. For example, in calculating turbulent flow about an airfoil at a chord Reynolds number of 10^6, grid spacings on the order of 10^{-4} chord may be required near the airfoil surface whereas spacings of the order of the airfoil chord may be permissible in the far field.

In considering possible airfoil coordinate systems, several candidate schemes are available. Among these candidates are conformal coordinate systems such as that used by Mehta (Ref. 20), systems based upon solution of Poisson's equation, and a constructive system (Refs. 31 and 60). Although conformal systems are excellent choices when they can be used, their very nature restricts their generality and hence they were not considered for the present effort.

A more general method is that of Thompson and his coworkers (e.g., Thompson, Thames and Mastin (Ref. 36)) which solves a Poisson equation to generate coordinates. Although this approach is considerably more general than the conformal approach, the generation of coordinates by this approach requires solution of a partial differential equation and obtaining a converged solution of Poisson's equation for general geometry can be a problem (Ref. 36). In addition difficulties may be encountered in obtaining a desirable distribution of grid points.

The third approach is that of constructing a coordinate system in which the required airfoil is by definition a coordinate line and in which grid point placement is specified by the user. Such a procedure was developed originally for the isolated airfoil problem by Gibeling, Shamroth and Eiseman (Ref. 31) and extended to the cascade problem by Eiseman (Ref. 60); it is this procedure which was used in the present calculations. To the authors' knowledge the present calculations represent the first successful attempt at solving the Navier-Stokes equations about an airfoil using a constructive coordinate system. The details of the constructive system are presented in Ref. 31 for an isolated airfoil and in Ref. 59 for a cascade.

RESULTS

NACA 0012 Airfoil at Zero Incidence

The first calculation presented is for a NACA 0012 airfoil at zero incidence. A highly stretched coordinate system was used for the calculations with grid spacing normal to the airfoil being of the order of .0005 c (where c is the chord) in the vicinity of the airfoil surface and of the order of 0.8 c at the outer grid boundary, approximately some three chords from the airfoil surface. The coordinate system was constructed using the method described in Refs. 31 and 60. The grid, which consisted of 41 x 30 points, extended approximately three chords upstream of the airfoil, three chords above and below the airfoil and six chords downstream of the airfoil. The dependent variables were the Cartesian velocity components, u and v, the density, ρ, and the turbulence kinetic energy, k. The governing equations were taken as the continuity equation, the momenta equations, and the turbulence kinetic energy equation. The independent variables for the turbulence kinetic energy equation were transformed from the Cartesian coordinates, x and y , in the same manner as the momenta and continuity equations were transformed from the Cartesian to the computational coordinates.

The calculation was initiated by specifying the inviscid solution throughout the flow field; applying zero velocity conditions on the airfoil surface and assuming a turbulence kinetic energy field. Boundary conditions were set as follows: on the airfoil surface the Cartesian velocities were set to zero and the boundary layer approximate transverse momentum equation ($\partial p/\partial n = 0$) used. At the outer boundary, velocity and density were set to the inviscid values for a Joukowski airfoil of approximately the same thickness whereas at the downstream boundary, first derivatives were set to zero along the coordinate direction approximately aligned with the free stream. A sketch of the boundaries is presented in Fig. 2. The turbulence kinetic energy equation was treated by setting, k, equal to a free stream turbulence level of 0.001 at the upstream outer boundary and setting the (nearly streamwise) derivative of k equal to zero at the downstream boundary. At the airfoil surface the correct condition on the turbulence kinetic energy should be k=0, however, the turbulence kinetic energy reaches a maximum very near the wall and then declines to zero (Ref. 61). Rather than try to include enough grid points in the near wall region to define

this sharp maximum and the subsequent decrease to zero at the wall an artificial boundary condition was applied in the spirit of the so-called wall function formulation. This boundary condition takes the form of setting the turbulence kinetic energy derivative at the wall equal to zero and thus not defining the decrease from the maximum k to the zero k wall condition. Obviously, an improved formulation would include enough points in the near wall region to adequately define the problem there and such an approach is expected to be followed in subsequent efforts.

The calculation was run in three steps. Initially a spatially varying turbulent viscosity field was specified and the mean flow equations were solved with these equations. During this part of the calculation since the transients were not of interest the equations were solved with the matrix conditioning approach developed by McDonald and Briley (Ref. 62) which results in a spatially varying time step. Matrix conditioning considerably accelerates the convergence of the mean flow equations to steady state. After the major flow readjustment had occurred the mean flow was "frozen" and the turbulence equations were solved. Finally all equations were solved and the flow development to steady state computed. Using this technique the solution reached convergence in approximately 150 time steps. Although other factors may be involved this result should be contrasted to the 800 time steps required by Steger (Ref. 34) to reach convergence in solving the thin shear layer equations.

A sketch of the predicted surface pressure distribution is presented in Fig. 3, which also shows the predictions of Mehta (Ref. 20) for laminar incompressible flow at Re_c = 10,000 and the data of Gregory and O'Reilly (Ref. 63) for turbulent flow at a Reynolds number of 2.88×10^6. In the present calculations the reference length, velocity, density, viscosity and temperature were chosen to obtain a Reynolds number based on chord of 10^6 and a Mach number of approximately 0.2. As can be seen in Fig. 3, both predictions are in good agreement with data over the forward portion of the airfoil. However, over the last 40% span, the measurements indicate substantially more recompression than either analysis predicts and, in fact, both analyses show good agreement with each other.

The suction surface pressure discrepancy between the analyses and the data deserves further comment. The trailing edge pressure predictions of Mehta's analysis were made with a coordinate grid which concentrated the available grid

points in the trailing edge as well as the leading edge regions. Thus the coordinate system used in the present analysis which obtains relatively high resolution in the leading edge region at the expense of some resolution in the trailing edge region does not seem to be the source of the discrepancy. However, it must be recalled that Mehta (Ref. 20) considered a laminar calculation whereas the Gregory and O'Reilly (Ref. 63) data is for turbulent flow. A laminar boundary layer is more susceptible to separation than a turbulent one and indeed, the prediction of Mehta (Ref. 20) does show separation upstream of the trailing edge whereas the data show the boundary layer to remain attached over the entire suction surface. Therefore the discrepancy between the data of Ref. 63 and the analysis of Mehta could be the result of the computed laminar boundary layer separating and modifying the trailing edge pressure distribution.

The present analysis however considers turbulent flow, but due to grid point limitations the boundary layer may not be sufficiently resolved for optimum results. Thus either the existing boundary layer resolution or perhaps the assumed turbulence model could cause the predicted boundary layer displacement effects to be larger than actually occur and this would result in a lower than expected pressure in the suction surface trailing edge region. This possible explanation is given some weight as a result of the second calculation presented in the present report. In this second calculation the zero incidence airfoil flow field was predicted using a grid having somewhat better resolution in the boundary layer region and the result was a higher prediction of trailing edge suction surface pressure. This will be discussed subsequently.

Isovel contours in the immediate vicinity of the airfoil surface for the zero incidence NACA 0012 case are presented in Fig. 4. The horizontal axis of the plot is x/c which is the dimensionless streamwise distance along the airfoil centerline. The vertical axis is the normal distance from the airfoil surface y_s/c. A sketch of these quantities is shown in the bottom portion of the figure. The contours in the vicinity of the leading edge stagnation point, $x/c = 0$, represent changes in the essentially inviscid velocity along the stagnation streamline, however, downstream of the leading edge region, $x/c > 0.1$, the isovels represent the viscous flow region and here the growth of the boundary layer is evident. The airfoil trailing edge is located at $x/c = 1.0$ and downstream of this location the isovels intersect the horizontal axis indicating the wake development.

Another view of the mean velocity field is shown in Fig. 5 which presents velocity profiles at various streamwise locations. The distances x/c and y_s/c are defined as in Fig. 4 and u/u_{ref} is the local velocity component in the x-direction divided by the velocity at upstream infinity. The dimensionless velocity reaches values greater than unity since the inviscid velocity at the edge of the boundary layer is greater than the velocity at upstream infinity. Although the flow approached a separated state at the trailing edge vicinity, separation never actually occurred; this could be due to the turbulent nature of the flow.

The calculated turbulence kinetic energy contours are presented in Fig. 6. The maximum predicted value of turbulence kinetic energy, $k = 0.06$, occurs at $x/c \approx 0.1$ and very close to the airfoil surface where the assumed wall function for turbulence kinetic energy was applied. Since these high values occur both in the wall function region and in the region where the flow was transitional (Fig. 7) this maximum value should be viewed with some skepticism. Further downstream, the values of k in the vicinity of the wall decreased to values between 0.02 and 0.04 which are more in keeping with experiment (Ref. 61). Turbulent viscosity isobars are presented in Fig. 7. Figure 7 indicates that transition occurs in the region $x/c \approx 0.2$ which is somewhat upstream of the region noted experimentally by Gregory and O'Reilly (Ref. 63). Further, according to Gregory and O'Reilly (Ref. 63) the transition location for flow about a NACA 0012 airfoil at $Re_c = 10^6$ is at $x/c = 0.4$. However, it must be recalled that the present turbulence model was applied without any 'tuning' and, hence the agreement is considered satisfactory for the present. As in Fig. 4, $x/c = 1.0$ represents the airfoil trailing edge and the wake is found downstream of this point.

The second case considered is again for an airfoil at zero incidence, however, in this case flow about a full airfoil rather than flow about half an airfoil with use of symmetry conditions was calculated. A constructive grid having 81 x 30 grid points was used. The flow conditions for this second case were a Reynolds number based upon chord of 10^6 and a Mach number of .147. In addition, the computational grid for this case was more highly stretched than for the previous case with the first grid point off the airfoil surface being located a distance of 0.0002 chords from the surface. When the full airfoil calculation is considered a major advantage of the constructive coordinate

grid becomes apparent. The Poisson generated coordinate system (Ref. 27) gives coordinate lines with discontinuous slope at the geometric centerline of the coordinate system emanating from the airfoil trailing edge, see Fig. 8, (the branch cut); the constructive coordinate system does not contain this problem. Therefore, performing a full airfoil calculation integration across the wake from the lower to upper boundary including the centerline point (e.g., line a-b on Fig. 8) presents no difficulty with the present coordinates. Although such a procedure is possible in a Poisson generated coordinate system, its implementation would require using a device such as one-sided differencing at the centerline or not solving the equations on the centerline but determining values there by extrapolation. One-sided differencing may lead to numerical difficulties and the extrapolation technique is equivalent to treating the centerline as a boundary and applying boundary conditions along this interior line. With either of these two devices the centerline would be treated in a special manner and, therefore, both of these devices are expected to be inferior to simply treating the centerline points as interior points in the manner of the present analysis.

The full airfoil calculation was made with function conditions applied for density and the two velocity components along the outer boundary line d-e-f-g-h. As for the symmetric half airfoil calculation the values were taken as the flow field values appropriate for a Joukowski airfoil of equal thickness. As in the first calculation the outer boundary was approximately three chords away from the airfoil surface. No slip conditions and zero density gradient conditions were applied at the airfoil surface and zero first derivative boundary conditions along the 'streamwise' direction for both velocity and density were applied at the outflow boundary.

The results of the full airfoil calculation are very similar to those of the half airfoil calculation presented in Figs. 3-7. The flow field is predicted to be symmetric about the centerline as is expected. The surface static pressure distribution shown in Fig. 9 is only slightly different from that shown in Fig. 3. The major difference being the higher pressure in the suction surface trailing edge region; this has been discussed previously and may be a result of the better boundary layer resolution in the full airfoil

calculation. Likewise the velocity, turbulence energy and turbulent viscosity fields differed little from those previously presented.

The third example considered is a NACA 0012 airfoil at 6° incidence. Again the Reynolds number based upon chord was 10^6 and the Mach number was 0.147. As in the previous example an 81x30 grid was used. In running the calculation some difficulty was experienced in bringing the transverse velocity, w, smoothly into the outer specified function boundary condition in the region d-e' and g'-h of Fig. 8. The initial attempt to resolve this problem focused upon the transverse grid which was very widely spaced in the vicinity of the outer loop, d-e'-f-g'-h. A new grid was constructed which sacrificed some minor amount of resolution in the boundary layer and even more resolution in the flow midregion to obtain better resolution near the outer loop. In this grid the first grid point off the airfoil was located a distance 0.00033 from the airfoil surface. Although this procedure decreased the oscillations in the w-component of velocity, it did not eliminate them; hence a second modification was made. In this modification the function boundary conditions on ρ, u and w along lines d-e and g-h (see Fig. 8) were replaced by specified static pressure and zero first derivatives of u and w; this set of boundary conditions removed the observed oscillations and the calculation proceeded without difficulty. Further this new set of boundary conditions appear more desirable from physical considerations. It should also be noted that the flexibility of the constructive coordinate in obtaining some desired mesh proved a very desirable property.

The predicted pressure distribution is compared with the data of Gregory and O'Reilly (Ref. 63) taken for a Reynolds number 2.8×10^6 in Fig. 10. As shown in Fig. 10 the major discrepancy between data and analytic prediction occurs in the leading edge region where the analysis fails to predict the correct suction peak. This discrepancy is at least partially a result of grid resolution. The strong favorable pressure gradient region leading to the suction peak occurs in a very limited region of the flow field between $x/c \approx 0$ and $x/c \approx 0.01$. This region extends over only one percent of the airfoil chord and only one tenth of one percent of the entire grid extent. In interest of computer run time economy the grid was limited to 81x30 points (a total of 2430 grid points) and even though points were packed into the leading edge region,

only four pseudo-radial lines were placed within the favorable pressure gradient region. Thus even with a total of 2430 grid points and severe leading edge grid packing, resolution in this region was marginal. It is expected that increased resolution would result in better agreement with the data.

A second area of moderate disagreement occurs in the trailing edge region; this results from differing predictions of trailing edge pressure. The discrepancy between predicted and measured trailing edge pressure also occurred in the zero incidence case and has been discussed previously in some detail. The lift distribution presented in the lower portion of Fig. 10 shows excellent agreement between data and analysis except in the region of the suction peak where as mentioned above the probable cause of disagreement is grid point resolution.

In regard to other aspects of the flow field the predicted suction surface transition location occurs at $x_T/c \approx 0.08$. The data of Gregory and O'Reilly gives $x_T \approx 0.04$ for a Reynolds number of 2.8×10^6 and $x_T/c \approx 0.08$ for a Reynolds number of 1.48×10^6. Thus the predicted transition location is in excellent agreement with data. The transition location predicted on the pressure surface is $x_T/c \approx 0.30$; thus the pressure surface boundary layer has a considerably longer laminar run than does the suction surface boundary layer. This result is as expected. The flow on the airfoil suction surface is subject to a very strong acceleration as it proceeds from the stagnation point around the airfoil leading edge and the large acceleration with resultant generation of large velocities is shown in Fig. 11. As the flow proceeds downstream, it encounters an adverse pressure gradient leading to a thickening of the boundary layer, typical adverse pressure boundary layer profiles and eventually separation at $x/c \approx .85$. The appearance of separation is at variance with the data of Gregory and O'Reilly (Ref. 63) taken at slightly higher Reynolds number which shows no separation at this incidence angle. However, the predicted separation region occurs on the very aft part of the airfoil and remains very small, thus having only a minor effect upon the generated pressure distribution. The difference between the analytic prediction of separation and the data may be due to any of several possibilities. Since the calculation was run at a slightly lower Reynolds number than the data, the difference may be due to Reynolds number effects. However, it is more likely that the discrepancy is tied to the

turbulence model; modification of the turbulence model structural functions could delay separation. Nevertheless, despite this difference the comparison between analytic prediction and experimental data is good. As is expected, the flow on the pressure surface is much less dramatic than that on the suction. The pressure surface has no suction peak and the boundary layer on the surface never encounters a strong adverse pressure gradient. The result is a well-behaved flow with no approach to separation. The suction surface and pressure surface boundary layers merge at the trailing edge where the wake is seen to be highly asymmetric.

A detailed picture of the flow in the leading edge region is presented in Fig. 12. In this figure the splitting of the flow as it encounters the airfoil, the appearance of the front stagnation and the large acceleration as the flow proceeds around the leading edge are all clearly pictured.

The turbulence energy field on both the suction and pressure surfaces is shown in Fig. 13. Since the regions of high turbulence energy are concentrated very near the airfoil surface, they are presented as lines of constant k on a plot of distance along airfoil surface to distance from airfoil surface as was done in Figs. 4, 6 and 7. The field shows distinctly different characteristics on the two different surfaces. On the suction surface large turbulence energies are generated in the region of the high adverse pressure gradient. However as the boundary layer proceeded in the high adverse pressure gradient region and approached separation, $x/c > 0.4$, the turbulence energy drops as a result of the low transverse velocity gradients associated with nearly separated boundary layers which can no longer produce turbulent energy. In fact on the aft portion of the airfoil suction surface the maximum turbulence energy appears away from the wall. The turbulence energy field on the pressure surface exhibits a different character. Although the field here does not generate as large k's as on the suction surface, relatively high turbulence levels are present over the entire surface flow field. Again this is to be expected since the boundary layer in this region does not approach separation.

CONCLUDING REMARKS

The present report describes a solution of the compressible, turbulent isolated airfoil flow field problem. The analysis used solves the full compressible Navier-Stokes equation via the consistently split linearized block implicit procedure of Briley and McDonald in a body-fitted constructive coordinate system. The constructive system has the airfoil surface as a coordinate line by definition and is capable of obtaining high grid resolution at user-specified regions of the flow field. To the author's knowledge the present results represent the first solution of the airfoil flow problem using the Navier-Stokes equations in conjunction with a constructive coordinate system.

Several forms of the Navier-Stokes equations are presented as possible candidates to obtain an accurate and efficient solution. Based upon a variety of considerations, including sample calculations of low Reynolds number flow about a circular cylinder, it is determined that the strong conservation form of the equations should not be solved; rather a form in which the geometric factors are not in conservative form is deemed superior for this problem.

Since high Reynolds number flow is the flow of interest, the present effort proposes a turbulence model based upon the turbulence kinetic energy equation with structural functions specified so as to be valid for laminar, transitional and fully turbulent flow. When used in conjunction with the mean flow equation, the model predicts a turbulence kinetic energy field, as well as a mean flow field. The analysis has been applied to high Reynolds number, subsonic Mach number flow about a NACA 0012 airfoil. At zero incidence the analysis gives a good comparison between the predicted airfoil static pressure distribution and experimental data. The only region which contains a discrepancy is the trailing edge region where grid resolution or turbulence modelling effects may give larger viscous displacement effects than were observed experimentally. In addition, the mean flow and turbulence energy results are as expected. Regions of laminar flow appear in the airfoil leading edge region and in regions distant from the airfoil. Transitional flow occurs near the airfoil surface in the quarter chord region and turbulent flow is predicted over the aft part of the airfoil and in the airfoil wake.

At 6 deg. incidence agreement between predicted and measured pressure distributions was again good except in the leading edge region where grid resolution problems prevented an accurate prediction of the suction peak. The predicted suction surface transition point was in excellent agreement with data and the mean and turbulence fields were qualitatively as expected.

Although some problems remain, particularly in regard to grid resolution and turbulence modelling, the results of the present analysis clearly show the capability of predicting the high Reynolds number isolated airfoil flow field in a constructive coordinate system including turbulence effects.

APPENDIX - THE NUMERICAL METHOD

Linearization Technique

A number of techniques have been used for implicit solution of the following first-order nonlinear scalar equation in one dependent variable $\phi(x,t)$:

$$\partial\phi/\partial t = F(\phi)\,\partial G(\phi)/\partial x \qquad \text{(A1)}$$

Special cases of Eq. (A1) include the conservation form if $F(\phi) = 1$, and quasi-linear flow if $G(\phi) = \phi$. Previous implicit methods for Eq. (A1) which employ nonlinear difference equations and also methods based on two-step predictor-corrector schemes are discussed by Ames (Ref. 64, p. 82) and von Rosenburg (Ref. 65), p. 56). One such method is to difference nonlinear terms directly at the implicit time level to obtain nonlinear implicit difference equations; these are then solved iteratively by a procedure such as Newton's method. Although otherwise attractive, there may be difficulty with convergence in the iterative solution of the nonlinear difference equations, and some efficiency is sacrificed by the need for iteration. An implicit predictor-corrector technique has been devised by Douglas and Jones (Ref. 66) which is applicable to the quasilinear case ($G = \phi$) of Eq. (A1). The first step of their procedure is to linearize the equation by evaluating the non-linear coefficient as $F(\phi^n)$ and to predict values of $\phi^{n+1/2}$ using either the backward difference or the Crank-Nicolson scheme. Values for ϕ^{n+1} are then computed in a similar manner using $F(\phi^{n+1/2})$ and the Crank-Nicolson scheme. Gourlay and Morris (Ref. 67) have also proposed implicit predictor-corrector techniques which can be applied to Eq. (A1). In the conservative case (F=1), their technique is to define $\dot{G}(\phi)$ by the relation $G(\phi) = \phi\dot{G}(\phi)$ when such a definition exists, and to evaluate $\dot{G}(\phi^{n+1})$ using the values for ϕ^{n+1} computed by an explicit predictor scheme. With $\dot{G}$ thereby known at the implicit time level, the equation can be treated as linear and corrected values of ϕ^{n+1} are computed by the Crank-Nicolson scheme.

A technique is described here for deriving linear implicit difference approximations for nonlinear differential equations. The technique is based on an expansion of nonlinear implicit terms about the solution at the known time

level, t^n, and leads to a one-step, two-level scheme which, being linear in unknown (implicit) quantities, can be solved efficiently without iteration. This idea was applied by Richtmyer and Morton (Ref. 68, p. 203) to a scalar nonlinear diffusion equation. Here, the technique is developed for problems governed by ℓ nonlinear equations in ℓ dependent variables which are functions of time and space coordinates. Although the present effort concentrates upon two spatial dimensions and time, the technique will be described for the three-dimensional, unsteady equations.

The solution domain is discretized by grid points having equal spacings in the computational coordinates, Δy^1, Δy^2 and Δy^3 in the y^1, y^2 and y^3 directions, respectively, and an arbitrary time step, Δt. The subscripts i, j, k and superscript n are grid point indices associated with y^1, y^2, y^3 and t, respectively, and thus $\phi^n_{i,j,k}$ denotes $\phi(y^1_i, y^2_j, y^3_k, t^n)$. It is assumed that the solution is known at the n level, t^n, and is desired at the (n+1) level, t^{n+1}. At the risk of an occasional ambiguity, one or more of the subscripts is frequently omitted, so that ϕ^n is equivalent to $\phi^n_{i,j,k}$.

Although present attention is focused on the compressible Navier-Stokes equations, the numerical method employed is quite general and is formally derived for systems of governing equations which have the following form:

$$\partial H(\phi)/\partial t = \mathcal{D}(\phi) + S(\phi) \tag{A2}$$

where ϕ is a column vector containing ℓ dependent variables, H and S are column vector functions of ϕ, and $\mathcal{D}$ is a column vector whose elements are spatial differential operators which may be multidimensional. The generality of Eq. (A2) allows the method to be developed concisely and permits various extensions and modifications (e.g., noncartesian coordinate systems, turbulence models) to be made more or less routinely. It should be emphasized, however, that the Jacobian $\partial H/\partial\phi$ must usually be nonsingular if the ADI techniques as applied to Eq. (A2) are to be valid. A necessary condition is that each dependent variable appear in one or more of the governing equations as a time derivative. An exception would occur if for instance, a variable having no time

derivative also appeared in only one equation, so that this equation could be decoupled from the remaining equations and solved a posteriori by an alternate method. As a consequence, the present method is not directly applicable to the incompressible Navier-Stokes equations except in one-dimension, where ADI techniques are unnecessary. For example, the velocity-pressure form of the incompressible equations has no time derivative of pressure, whereas the vorticity-stream-function form has no time derivative of stream function. For computing steady solutions, however, the addition of suitable "artificial" time derivatives to the incompressible equations, as was done in Chorin's (Ref. 69) artificial compressibility method, would permit the application of the present method. Alternatively, a low Mach number solution of the compressible equations can be computed.

The linearized difference approximation is derived from the following implicit time-difference replacement of Eq. (A2):

$$(H^{n+1} - H^n)/\Delta t = \beta\left[\mathcal{D}(\phi^{n+1}) + S^{n+1}\right] + (1-\beta)\left[\mathcal{D}(\phi^n) + S^n\right] \tag{A3}$$

where, for example, $H^{n+1} \equiv H(\phi^{n+1})$. The form of $\mathcal{D}$ and the spatial differencing are as yet unspecified. A parameter $\beta (0 \leq \beta \leq 1)$ has been introduced so as to permit a variable centering of the scheme in time. Equation (A3) produces a backward difference formulation for $\beta = 1$ and a Crank-Nicolson formulation for $\beta = 1/2$.

The linearization is performed by a two-step process of expansion about the known time level t^n and subsequent approximation of the quantity $(\partial\phi/\partial t)^n \Delta t$, which arises from chain rule differentiation, by $(\phi^{n+1} - \phi^n)$. The result is

$$H^{n+1} = H^n + (\partial H/\partial \phi)^n (\phi^{n+1} - \phi^n) + O(\Delta t)^2 \tag{A4a}$$

$$S^{n+1} = S^n + (\partial S/\partial \phi)^n (\phi^{n+1} - \phi^n) + O(\Delta t)^2 \tag{A4b}$$

$$\mathcal{D}(\phi^{n+1}) = \mathcal{D}(\phi^n) + (\partial \mathcal{D}/\partial\phi)^n(\phi^{n+1} - \phi^n) + O(\Delta t)^2 \tag{A4c}$$

The matrices $\partial H/\partial\phi$ and $\partial S/\partial\phi$ are standard Jacobians whose elements are defined, for example, by $(\partial H/\partial\phi)_{qr} \equiv \partial H_q/\partial\phi_r$. The operator elements of the matrix $\partial\mathcal{D}/\partial\phi$ are similarly ordered, i.e., $(\partial\mathcal{D}/\partial\phi)_{qr} \equiv \partial\mathcal{D}_q/\partial\phi_r$; however, the intended meaning of the operator elements requires some clarification. For the q^{th} row, the operation $(\partial\mathcal{D}_q/\partial\phi)^n\,(\phi^{n+1} - \phi^n)$ is understood to mean that $\{\partial/\partial t\,\mathcal{D}_q[\phi(x,y,z,t)]\}^n\,\Delta t$ is computed and that all occurrences of $(\partial\phi_r/\partial t)^n$ arising from chain rule differentiation are replaced by $(\phi_r^{n+1} - \phi_r^n)/\Delta t$.

After linearization as in Eqs. (A4), Eq. (A3) becomes the following linear implicit time-differenced scheme:

$$(\partial H^n/\partial\phi)(\phi^{n+1} - \phi^n)/\Delta t = \mathcal{D}(\phi^n) + S^n + \beta\,(\partial\mathcal{D}/\partial\phi + \partial S^n/\partial\phi)(\phi^{n+1} - \phi^n) \tag{A5}$$

Although H^{n+1} is linearized to second order in Eq. (A4), the division by Δt in Eq. (A3) introduces an error term of order Δt. A technique for maintaining formal second-order accuracy in the presence of nonlinear time derivatives is discussed by McDonald and Briley (Ref. 70), however, a three-level scheme results. Second-order temporal accuracy can also be obtained (for $\beta = 1/2$) by a change in dependent variable to $\hat{\phi} \equiv H(\phi)$, provided this is convenient, since the nonlinear time derivative is then eliminated. The temporal accuracy is independent of the spatial accuracy.

On examination, it can be seen that Eq. (A5) is linear in the quantity $(\phi^{n+1} - \phi^n)$ and that all other quantities are either known or evaluated at the n level. Computationally, it is convenient to solve Eq. (A5) for $(\phi^{n+1} - \phi^n)$ rather than ϕ^{n+1}. This both simplifies Eq. (A5) and reduces roundoff errors, since it is presumably better to compute a small $O(\Delta t)$ change in an $O(1)$ quantity than the quantity itself. To simplify the notation, a new dependent variable ψ defined by

$$\psi \equiv \phi - \phi^n \tag{A6}$$

is introduced, and thus $\psi^{n+1} = \phi^{n+1} - \phi^n$, and $\psi^n = 0$. It is also convenient to rewrite Eq. (A5) in the following simplified form:

$$(A + \Delta t\, \mathcal{L})\psi^{n+1} = \Delta t \left[\mathcal{D}(\phi^n) + S^n\right] \tag{A7a}$$

where the following symbols have been introduced to simplify the notation:

$$A \equiv \partial H^n / \partial \phi - \beta \Delta t (\partial S^n / \partial \phi) \tag{A7b}$$

$$\mathcal{L} \equiv -\beta (\partial \mathcal{D} / \partial \phi) \tag{A7c}$$

It is noted that $\mathcal{L}(\psi)$ is a linear transformation and thus $\mathcal{L}(0) = 0$. Furthermore, if $\mathcal{D}(\phi)$ is linear, then $\mathcal{L}(\psi) = -\beta\, \mathcal{D}(\psi)$.

Spatial differencing of Eq. (A7a) is accomplished simply by replacing derivative operators such as $\partial/\partial y^i$, $\partial^2/\partial y^i \partial y^i$ by corresponding finite difference operators, D_i, D_i^2. Henceforth, it is assumed that $\mathcal{D}$ and $\mathcal{L}$ have been discretized in this manner, unless otherwise noted.

Before proceeding, some general observations seem appropriate. The foregoing linearization technique assumes only Taylor expandability, an assumption already implicit in the use of a finite difference method. The governing equations and boundary conditions are addressed directly as a system of coupled nonlinear equations which collectively determine the solution. The approach thus seems more natural than that of making ad hoc linearization and decoupling approximations, as is often done in applying implicit schemes to coupled and/or nonlinear partial differential equations. With the present approach, it is not necessary to associate each governing equation and boundary condition with a particular dependent variable and then to identify various "nonlinear coefficients" and "coupling terms" which must then be treated by lagging, predictor-corrector techniques, or iteration. The Taylor expansion procedure is analogous to that used in the generalized Newton-Raphson or quasi-linearization

methods for iterative solution of nonlinear systems by expansion about a known current guess at the solution (e.g., Bellman & Kalaba, Ref. 71). However, the concept of expanding about the previous time level apparently had not been employed to produce a noniterative implicit time-dependent scheme for coupled equations, wherein nonlinear terms are approximated to a level of accuracy commensurate with that of the time differencing. The linearization technique also permits the implicit treatment of coupled nonlinear boundary conditions, such as stagnation pressure and enthalpy at subsonic inlet boundaries, and in practice, this latter feature was found to be crucial to the stability of the overall method (Ref. 40).

Application of Alternating-Direction Techniques

Solution of Eq. (A7a) is accomplished by application of an alternating-direction implicit (ADI) technique for parabolic-hyperbolic equations. The original ADI method was introduced by Peaceman and Rachford (Ref. 72) and Douglas (Ref. 73); however, the alternating-direction concept has since been expanded and generalized. A discussion of various alternating-direction techniques is given by Mitchell (Ref. 74) and Yanenko (Ref. 39).

The present technique is simply an application of the very general procedure developed by Douglas and Gunn (Ref. 41) for generating ADI schemes as perturbations of fundamental implicit difference schemes such as the backward-difference or Crank-Nicolson schemes.

For the present, it will be assumed that $\mathcal{D}(\phi)$ contains derivatives of first and second order with respect to y^1, y^2 and y^3, but no mixed derivatives. In this case, $\mathcal{D}$ can be split into three operators, $\mathcal{D}_1, \mathcal{D}_2, \mathcal{D}_3$ associated with the y^1, y^2 and y^3 coordinates and each having the functional form $\mathcal{D}_i = \mathcal{G}(\phi, \partial/\partial y^i, \partial^2/\partial y^i \partial y^i)$. Equation (A7a) then becomes

$$\left[A + \Delta t(\mathcal{L}_1 + \mathcal{L}_2 + \mathcal{L}_3)\right]\psi^{n+1} = \Delta t\left[(\mathcal{D}_1 + \mathcal{D}_2 + \mathcal{D}_3)\phi^n + S^n\right] \tag{A8}$$

Recalling that $\mathcal{L}(\psi^n) = 0$, the Douglas-Gunn representation of Eq. (A8) can be written as the following three-step solution procedure:

$$(A+\Delta t\,\mathcal{L}_1)\psi^* = \Delta t\left[(\mathcal{D}_1+\mathcal{D}_2+\mathcal{D}_3)\phi^n+S^n\right] \tag{A9a}$$

$$(A+\Delta t\,\mathcal{L}_2)\psi^{**} = A\psi^* \tag{A9b}$$

$$(A+\Delta t\,\mathcal{L}_3)\psi^{n+1} = A\psi^{**} \tag{A9c}$$

where ψ^* and ψ^{**} are intermediate solutions. It will be shown subsequently that each of Eqs. (A9) can be written in narrow block-banded matrix form and solved by efficient block-elimination methods. If ψ^* and ψ^{**} are eliminated, Eqs. (A9) become

$$(A+\Delta t\,\mathcal{L}_1)A^{-1}(A+\Delta t\,\mathcal{L}_2)A^{-1}(A+\Delta t\,\mathcal{L}_3)\psi^{n+1} = \Delta t\left[(\mathcal{D}_1+\mathcal{D}_2+\mathcal{D}_3)\phi^n+S^n\right] \tag{A10}$$

If the multiplication on the left-hand side of Eq. (A10) is performed, it becomes apparent that Eq. (A10) approximates Eq. (A8) to order $(\Delta t)^2$. Although the stability of Eqs. (A9) has not been established in circumstances sufficiently general to encompass the Navier-Stokes equations, it is often suggested (e.g., Richtmyer & Morton, Ref. 68, p. 215) that the scheme is stable and accurate under conditions more general than those for which rigorous proofs are available. This latter notion was adopted here as a working hypothesis supported by favorable results obtained in actual computations (e.g., Ref. 38).

A major attraction of the Douglas-Gunn scheme is that the intermediate solutions ψ^* and ψ^{**} are consistent approximations to ψ^{n+1}. Furthermore, for steady solutions, $\psi^n = \psi^* = \psi^{**} = \psi^{n+1}$ independent of Δt. Thus, physical boundary conditions for ψ^{n+1} can be used in the intermediate steps without a serious loss in accuracy and with no loss for steady solutions. In this respect, the Douglas-Gunn scheme appears to have an advantage over locally one-dimensional (LOD) or "splitting" schemes, and other schemes whose intermediate steps do not satisfy the consistency condition. The lack of consistency in the intermediate steps complicates the treatment of boundary conditions and, according to Yanenko

(Ref. 39, p. 33), does not permit the use of asymptotically large time steps. It is not clear that this advantage of the Douglas-Gunn scheme would always outweigh other benefits which might be derived from an alternative scheme. However, since the ADI scheme can be viewed as an approximate technique for solving the fundamental difference scheme, Eq. (A7a), alternate techniques can readily be used within the present formulation.

It is worth noting that the operator $\mathcal{D}$ can be split into any number of components which need not be associated with a particular coordinate direction. As pointed out by Douglas and Gunn (Ref. 41), the criterion for identifying sub-operators is that the associated matrices be "easily solved" (i.e., narrow-banded). Thus, mixed derivatives can be treated implicitly within the ADI framework, although this would increase the number of intermediate steps and thereby complicate the solution procedure. Finally, only minor changes are introduced if, in the foregoing development of the numerical method, H, $\mathcal{D}$, and S are functions of the spatial coordinates and time, as well as ϕ.

Solution of the Implicit Difference Equations

Since each of Eqs. (A9) is implicit in only one coordinate direction, the solution procedure can be discussed with reference to a one-dimensional problem. For simplicity, it is sufficient to consider Eq. (A9a) with $\mathcal{D}_2, \mathcal{D}_3 \equiv 0$. Consider the following three-point difference formulas:

$$D_{\tilde{x}}\phi \equiv \left[\alpha \Delta_- + (1-\alpha)\Delta_+\right]\phi/\Delta\tilde{x} = (\partial\phi/\partial\tilde{x})_i + O\left[\Delta\tilde{x}^2 + (\alpha - 1/2)\Delta\tilde{x}\right] \qquad \text{(A11a)}$$

$$D_{\tilde{x}}^2\phi \equiv (\Delta_+\Delta_-)\phi/(\Delta\tilde{x})^2 = (\partial^2\phi/\partial\tilde{x}^2)_i + O(\Delta\tilde{x}^2) \qquad \text{(A11b)}$$

for a typical computational coordinate $\tilde{x}$. Here, $\Delta_- \equiv \phi_i - \phi_{i-1}$, $\Delta_+ \equiv \phi_{i+1} - \phi_i$, and a parameter α has been introduced ($0 \leq \alpha \leq 1$) so as to permit continuous variation from backward to forward differences. The standard central difference formula is recovered for $\alpha = 1/2$.

As an example, suppose that the q^{th} component of $\mathcal{D}_x^-$ has the form

$$\mathcal{D}_{xq}(\phi) = F_{1q}^T(\phi)\frac{\partial}{\partial \tilde{x}} G_{1q}(\phi) + F_{2q}^T(\phi)\frac{\partial^2}{\partial \tilde{x}^2} G_{2q}(\phi) \tag{A12}$$

where F and G are column vector functions having the same but an arbitrary number of components; F^T denotes the transpose of F. The form of Eq. (A12) permits governing equations having any number of first and second derivative terms. Then,

$$\Delta t \frac{\partial \mathcal{D}_{xq}}{\partial t} \simeq \frac{\partial \mathcal{D}_{xq}}{\partial \phi}(\phi^{n+1} - \phi^n) \equiv \left[F_{1q}^T \frac{\partial}{\partial \tilde{x}} \frac{\partial G_{1q}}{\partial \phi} + \frac{\partial G_{1q}^T}{\partial \tilde{x}} \frac{\partial F_{1q}}{\partial \phi}\right]^n (\phi^{n+1} - \phi^n)$$

$$+ \left[F_{2q}^T \frac{\partial^2}{\partial \tilde{x}^2} \frac{\partial G_{2q}}{\partial \phi} + \frac{\partial^2 G_{2q}^T}{\partial \tilde{x}^2} \frac{\partial F_{2q}}{\partial \phi}\right]^n (\phi^{n+1} - \phi^n) \tag{A13}$$

It is now possible to describe the solution procedure for Eq. (A9a) for the one-dimensional case with $\mathcal{D}_x^-$ given by Eq. (A12) and appropriate difference formulas. Because of the spatial difference operators, D_x^- and D_x^{-2}, Eq. (A9a) contains ψ^*_{i-1}, ψ^*_i, and ψ^*_{i+1}; consequently, the system of linear equations generated by writing Eq. (A9a) at successive grid points x_i can be written in block-tridiagonal form (simple tridiagonal for scalar equations, $\ell = 1$). The block-tridiagonal matrix structure emerges from rewriting Eq. (A9a) as

$$a_i^n \psi^*_{i-1} + b_i^n \psi^*_i + c_i^n \psi^*_{i+1} = d_i^n \tag{A14}$$

where a, b, c are matrices and d is a column vector, each containing only n-level quantities. When applied at successive grid points, Eq. (A14) generates a block-tridiagonal system of equations for ψ^* which, after appropriate treatment of boundary conditions, can be solved efficiently using standard block-elimination methods as discussed by Isaacson and Keller (Ref. 75, p. 58). The solution procedure for Eqs. (A9b&c) is analogous to that just described for Eq. (A9a). It is worth noting that the spatial difference parameter α can be varied with i or even term by term. For example, an "upwind difference" formula can be obtained if α is chosen as 1 or -1 depending on the sign of the elements of F_1.

REFERENCES

1. Kreskovsky, J. P.; Shamroth, S. J.; and Briley, W. R.: A Numerical Study of the Unsteady Leading Edge Separation Bubble on an Oscillating Airfoil. Computer Methods in Applied Mechanics and Engineering, vol. 11, no. 1, April 1977, pp. 39-56.

2. Shamroth, S. J.; and Kreskovsky, J. P.: A Weak Interaction Study of the Viscous Flow about Oscillating Airfoils. NASA CR-132425, 1974.

3. Briley, W. R.; and McDonald, H.: Numerical Prediction of Incompressible Separation Bubbles. J. Fluid Mech., vol. 69, part 4, 1975, pp. 631-656.

4. Velkoff, H. R.; Blaser, D. A.; and Jones, K. M.: Boundary Layer Discontinuity on a Helicopter Rotor Blade in Hovering. Journal of Aircraft, vol. 8, 1971, pp. 101-107.

5. Isogai, K.: An Experimental Study of the Unsteady Behavior of an Airfoil During Dynamic Stall with Special Reference to the Mechanism of the Stall Overshoot Effect. MIT ASRL TR-130-2, June 1970.

6. McCroskey, W. J.; and Philippe, J. J.: Unsteady Viscous Flow on Oscillating Airfoils. AIAA Paper 74-182, 1974.

7. McCroskey, W. J.; Carr, L. W.; and McAlister, K. W.: Dynamic Stall Experiments on Oscillating Airfoils. AIAA Journal, vol. 14, no. 1, January 1976, pp. 57-63.

8. Parker, A. G.: Force and Pressure Measurements on an Airfoil Oscillating through Stall. J. Aircraft, vol. 13, no. 10, October 1976, pp. 823-827.

9. Proceedings of the AGARD Conference on Unsteady Aerodynamics, AGARD CP-227, September 1977.

10. Saxena, L.S.; Fejer, A. A.; and Morkovin, M. V.: Features of Unsteady Flows Over Airfoils. Proceedings of AGARD Conference on Unsteady Aerodynamics, September 1977.

11. Philippe, J. J.: Le Decrochage Dynamique. Un Example D'Interaction Forte Entre Ecoulements Visqueux Et Non-Visqueux. Proceedings of AGARD Conference on Unsteady Aerodynamics, September 1977.

12. McCroskey, W. J.: Some Current Research on Unsteady Fluid Dynamics - 1976 Freeman Scholar Lecture. J. Fluids Eng., vol. 99, March 1977, pp. 8-39.

13. Ham, N. D.; and Garelick, M. S.: Dynamic Stall Considerations in Helicopter Rotors. J. American Helicopter Soc., vol. 13, no. 2, April 1968, pp. 49-55.

14. Bandu, N.; Sagner, M.; and Souquet, J.: Modelisation du Decrochage Dynamique d'un Profil Oscillant. AAAF 10th Colluque d'Aerodynamique Appliquee, Lille, France, November 1973.

15. Carta, F. O.; Commerford, G. L.; and Carlson, R. G.: Determination of Airfoil and Rotor Blade Dynamic Stall Response. J. American Helicopter Soc., vol. 18, no. 2, 1973, pp. 31-39.

16. Ericsson, L. E.; and Reding, J. P.: Dynamic Stall Analysis in Light of Recent Numerical and Experimental Results. AIAA Preprint No. 75-26, 1975.

17. Lang, J. D.: A Model for the Dynamics of a Separation Bubble Used to Analyze Control-Surface Buzz and Dynamic Stall. AIAA Paper 75-867, 1975.

18. Crimi, P.; and Reeves, B. L.: A Method for Analyzing Dynamic Stall of Helicopter Rotor Blades. NASA CR-2009, May 1972.

19. Mehta, U. B.; and Lavan, Z.: Starting Vortex, Separation Bubble and Stall: A Numerical Study of Laminar Unsteady Flow About an Airfoil. J. Fluid Mech., vol. 67, 1975, pp. 227-256.

20. Mehta, U. B.: Dynamic Stall of an Oscillating Airfoil. Proceedings of AGARD Conference on Unsteady Aerodynamics, September 1977.

21. Wu, J. C.; and Sampath, S.: A Numerical Study of Viscous Flow About an Airfoil. AIAA Paper 76-337, 1976.

22. Wu, J. C.; Sampath, S.; and Sankar, N. L.: A Numerical Study of Unsteady Viscous Flows around Airfoils. Proceedings of AGARD Conference on Unsteady Aerodynamics, September 1977.

23. Wu, J. C.; and Thompson, J. F.: Numerical Solutions of Time-Dependent Incompressible Navier-Stokes Equations Using an Integro-Differential Formulation. Computers and Fluids, vol. 1, 1973, pp. 197-215.

24. Kinney, R. B.; and Cielak, Z. M.: Analysis of Unsteady Viscous Flow Past an Airfoil: Part I - Theoretical Development. AIAA Journal, vol. 15, no. 12, December 1977, pp. 1714-1719.

25. Cielak, Z. M.; and Kinney, R. B.: Analysis of Unsteady Viscous Flow Past an Airfoil: Part II - Numerical Formulation and Results. AIAA Journal, vol. 16, no. 2, February 1978, pp. 105-110.

26. Hodge, J.K.; and Stone, A. L.: Numerical Solution for Airfoils Near Stall in Optimized Body Fitted Curvilinear Coordinates. AIAA Paper 78-284, 1978.

27. Thompson, J. F.; Thames, F. C.; and Mastin, C. W.: Boundary Fitted Curvilinear Coordinate Systems for Solution of Partial Differential Equations on Fields Containing Any Number of Arbitrary Two-Dimensional Bodies. NASA CR-2729, July 1977.

28. Verhoff, A.: Numerical Solution of Subsonic Viscous Inviscid Interacting Flows. AFFDL-TR-76-64, July 1976.

29. Deiwert, G. S.: Recent Computation of Viscous Effects in Transonic Flow. Proceedings of the Fifth International Conference on Numerical Methods in Fluid Dynamics, Springer-Verlag, New York, 1976.

30. Levy, L. L., Jr.: An Experimental and Computational Investigation of the Steady and Unsteady Transonic Flow Fields about an Airfoil in a Solid Wall Test Channel. AIAA Paper 77-678, 1977.

31. Gibeling, H. J.; Shamroth, S. J.; and Eiseman, P. R.: Analysis of Strong-Interaction Dynamic Stall for Laminar Flow on Airfoils. NASA CR-2969, April 1978.

32. MacCormack, R. W.: The Effect of Viscosity in Hypervelocity Impact Cratering. AIAA Paper No. 69-354, 1967.

33. MacCormack, R. W.: An Efficient Explicit-Implicit Characteristic Method for Solving the Compressible Navier-Stokes Equations. SIAM-AMS Proceedings of the Symposium on Computational Fluid Dynamics, 1977.

34. Steger, J. L.: Implicit Finite Difference Simulation of Flow About Arbitrary Geometries with Application to Airfoils. AIAA Paper 77-665, 1977.

35. Steger, J. L.: Implicit Finite Difference Simulation of Flow About Arbitrary Two-Dimensional Geometries. AIAA Journal, vol. 16, 1978, pp. 679-686.

36. Thompson, J. F.; Thames, F. C.; and Mastin, C. W.: Automatic Numerical Generation of Body Fitted Curvilinear Coordinate System for Field Containing Any Number of Arbitrary Two-Dimensional Bodies. J. Comp. Physics, vol. 15, 1974, pp. 299-319.

37. Beam, R.; and Warming, R. F.: An Implicit Finite Difference Algorithm for Hyperbolic Systems in Conservation-Law-Form. J. Comp. Physics, vol. 22, September 1976, pp. 87-110.

38. Briley, W. R.: and McDonald, H.: Solution of the Multidimentional Compressible Navier-Stokes Equations by a Generalized Implicit Method. J. Comp. Physics, vol. 24, no. 4, August 1977, p. 372.

39. Yanenko, N. N.: The Method of Fractional Steps, Springer-Verlag, New York, 1971.

40. Briley, W. R.; and McDonald, H.: On the Structure and Use of Linearized Block ADI and Related Schemes. J. Comp. Physics (Accepted for publication)

41. Douglas, J.; and Gunn, J. E.: A General Formulation of Alternating Direction Methods. Numerische Math., Vol. 6, 1964, pp. 428-453.

42. Pai, S. I.: Viscous Flow Theory - Vol. I Laminar Flow. Van Nostrand Co., Princeton, 1956.

43. Schlichting, H.: Boundary Layer Theory. McGraw Hill Co., New York, 1960.

44. McVittie, G. C.: A Systematic Treatment of Moving Axes in Hydrodynamics. Proceedings of the Royal Society A, 196, pp. 285-300.

45. Walkden, F.: The Equations of Motion of a Viscous, Compressible Gas Referred to an Arbitrarily Moving Coordinate System. Royal Aircraft Establishment, Technical Report No. 66140, April 1966.

46. Shamroth, S. J.; and Gibeling, H. J.: Computations with the Navier-Stokes Equations in Non-Cartesian Geometries. Scientific Research Associates Report R78-5, 1978.

47. McDonald, H.; and Fish, R. W.: Practical Calculation of Transitional Boundary Layers. Int. J. Heat and Mass Transfer, vol. 16, no. 9, 1973, pp. 1729-1744.

48. Shamroth, S. J.; and McDonald, H.: Assessment of a Transitional Boundary Layer Theory at Low Hypersonic Mach Numbers. Int. J. Heat and Mass Transfer, vol. 18, 1975, pp. 1277-1284.

49. Kreskovsky, J. P.; Shamroth, S. J.; and McDonald, H.: Application of a General Boundary Layer Analysis to Turbulent Boundary Layers Subjected to Strong Favorable Pressure Gradients. J. Fluid Eng., vol. 97, June 1975, pp. 217-224.

50. Jones, W. P.; and Launder, B. E.: Some Properties of Sink Flow Turbulent Boundary Layer. J. Fluid Mech., vol. 46, 1972, pp. 337-351.

51. Launder, B. E.; and Jones, W. P.: Sink Flow Turbulent Boundary Layers. J. Fluid Mech., vol. 38, 1969, pp. 817-831.

52. Pridden, C. H.: The Behavior of the Turbulent Boundary Layer on Curved Porous Walls. Ph.D. Thesis, University of London, 1974.

53. Launder, B. E.; and Spalding, D. B.: The Numerical Computation of Turbulent Flows. Computer Methods in Applied Mechanics and Engineering, vol. 3, 1974, pp. 269-289.

54. Quemard, C.; and Michel, R.: Definition and Application of Means For Predicting Shear Turbulent Flows in Turbomachines. ASME Paper 76-GT-67, 1976.

55. Favre, A. J.: The Equations of Compressible Turbulent Gases. Annual Summary Report No. 1, Institute de Mechanique Statistique de la Turbulence, January 1965.

56. Gibeling, H. J.; McDonald, H.; and Briley, W. R.: Development of a Three-Dimensional Combustor Flow Analysis, Vols. I and II: Theoretical Studies. Air Force Aero Propulsion Laboratory Report AFAPL-TR-75-59; vol. I, July 1975, vol. II, October 1976.

57. McDonald, H.: Combustion Modelling in Two and Three Dimensions. Progress in Combustion and Energy Science. Pergamon Press, New York. (Accepted for publication)

58. Briley, W. R.; McDonald, H.; and Gibeling, H. J.: Solution of the Multidimensional Compressible Navier-Stokes Equations by a Generalized Implicit Method. United Technologies Research Center Report R76-911363-15, January 1976.

59. Levy, R.; Shamroth, S. J.; Gibeling, H. J.; and McDonald, H.: A Study of the Turbulent Shock Wave Boundary Layer Interaction. Air Force Flight Dynamics Laboratory Report AFFDL-TR-76-163, February 1977.

60. Eiseman, P. R.: A Coordinate System for a Viscous Transonic Cascade Analysis. J. Comp. Physics, vol. 26, March 1978, pp. 307-338.

61. Hinze, J.: Turbulence. McGraw Hill Co., New York, 1959.

62. McDonald, H.; and Briley, W. R.: Computational Fluid Dynamics Aspects of Internal Flows. AIAA Paper 79-1445, 1979.

63. Gregory, N.; and O'Reilly, C. L.: Low Speed Aerodynamic Characteristics of NACA 0012 Airfoil Section, Including the Effects of Upper Surface Roughness Simulating Hoarfrost. Aero Report 1308, National Physics Laboratory, 1970.

64. Ames, W. F.: Numerical Methods for Partial Differential Equations. Barnes & Noble, Inc., New York, New York, 1969.

65. von Rosenberg, D. A.: Methods for the Numerical Solution of Partial Differential Equations. American Elsevier Publishing Co., Inc., New York, New York, 1969.

66. Douglas, J.; and Jones, B. F.: On Predictor-Corrector Methods for Nonlinear Parabolic Differential Equations. Soc. for Indust. Appl. Math., Vol. 11, 1963, pp. 195-204.

67. Gourlay, A. R.; and Morris, J. L.: Finite-Difference Methods for Nonlinear Hyperbolic Systems. Math. Comp., Vol. 22, 1968, pp. 28-39.

68. Richtmyer, R. D.; and Morton, K. W.: Difference Methods for Inital Value Problems. Second Edition. Interscience Publishers, New York, New York, 1967.

69. Chorin, A. J.: Numerical Study of Thermal Convection in a Fluid Layer Heated from Below. AEC R&D Report TID-4500 (also New York Univ. Report NYO-1480-61), 1966.

70. McDonald, H.; and Briley, W. R.: Three-Dimensional Supersonic Flow of a Viscous or Inviscid Gas. J. Comp. Physics, Vol. 19, No. 2, October 1975, p. 150.

71. Bellman, R. E.; and Kalaba, R. E.: Quasilinearization and Nonlinear Boundary-Value Problems. American Elsevier Publ. Co., Inc., New York, 1965.

72. Peaceman, D. W.; and Rachford, H. H.: The Numerical Solution of Parabolic and Elliptic Differential Equations. Soc. for Indust. Appl. Math., Vol. 3, 1955, pp. 28-41.

73. Douglas, J.: On the Numerical Integration of $u_{xx} + u_{yy} = u_t$ by Implicit Methods. Soc. for Indust. Appl. Math., Vol. 3, 1955, pp. 42-65.

74. Mitchell, A. R.: Computational Methods in Partial Differential Equations. John Wiley and Sons, Inc., New York, 1969.

75. Isaacson, E.; and Keller, H. B.: Analysis of Numerical Methods. John Wiley and Sons, Inc., New York, 1966.

76. Son, J. S.; and Hanratty, T. J.: Numerical Solution for the Flow Around a Circular Cylinder at Reynolds Numbers of 40, 200 and 500. J. Fluid Mech., Vol. 35, 1969, pp. 369-386.

77. Kawaguti, M.: Numerical Solution of the Navier-Stokes Equations for the Flow Around a Circular Cylinder at Reynolds Number 40. J. Phys. Soc. of Japan, Vol. 8, 1953, pp. 747-757.

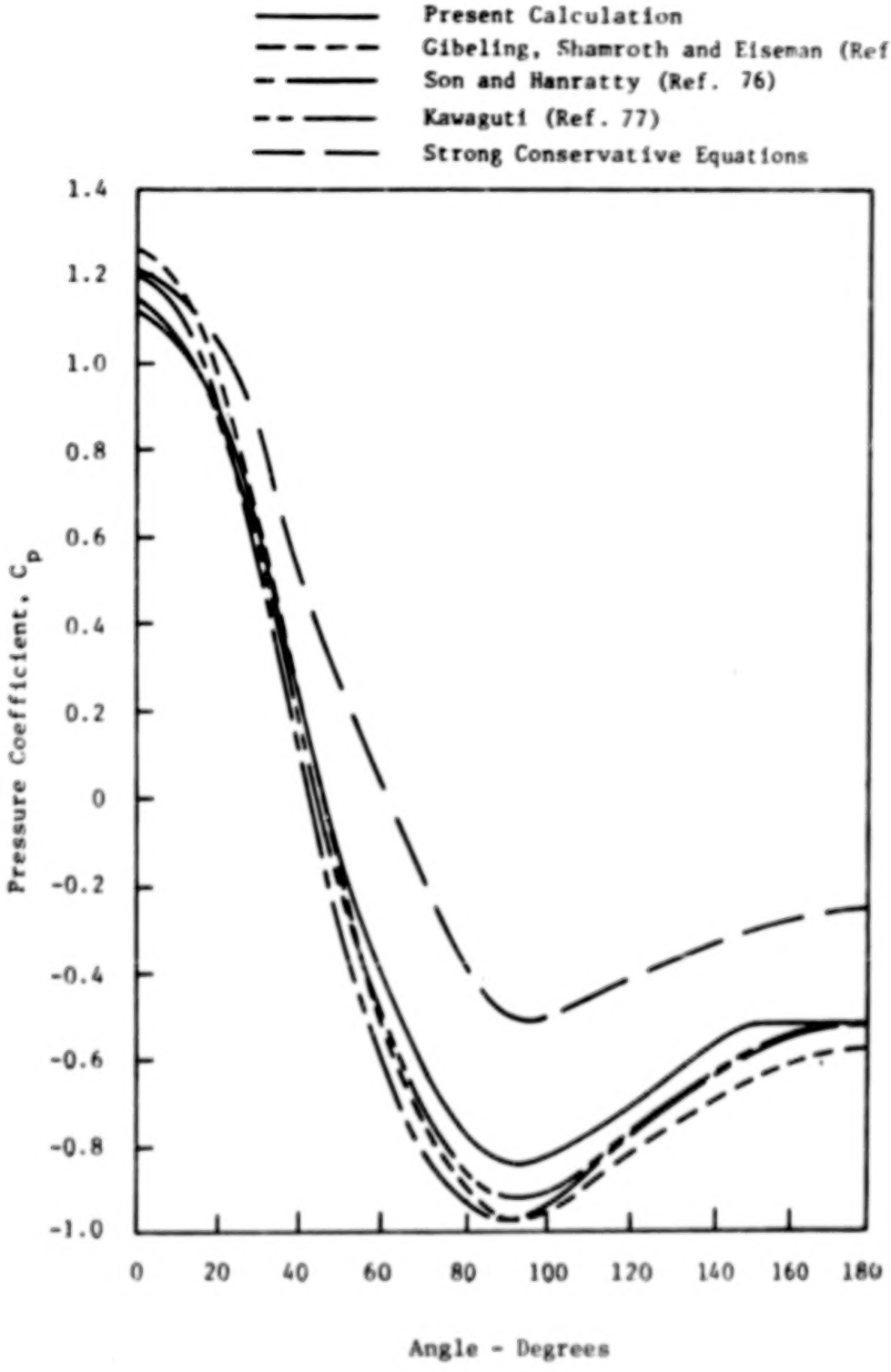

Figure 1. - Pressure distribution about circular cylinder, $Re_D = 40$.

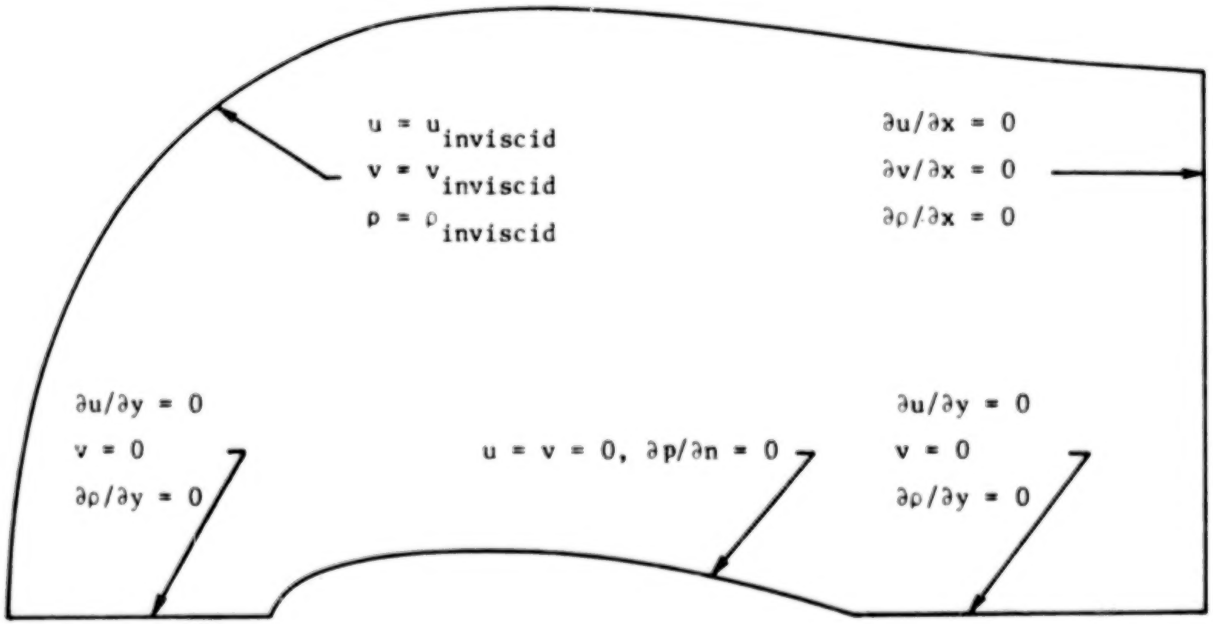

Figure 2. - Sketch detailing boundary conditions.

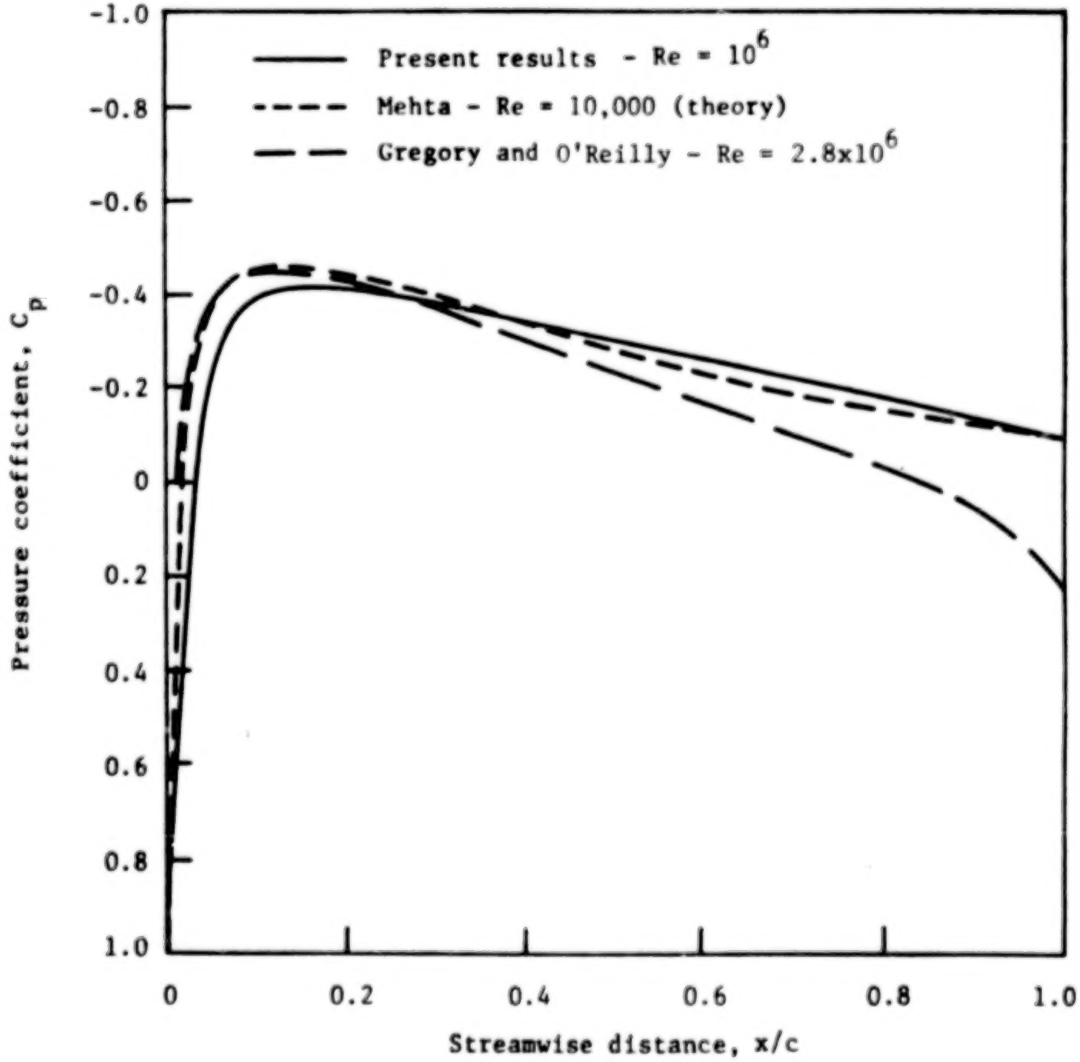

Figure 3. - Surface pressure distribution for NACA 0012 airfoil at zero incidence (half airfoil calculation).

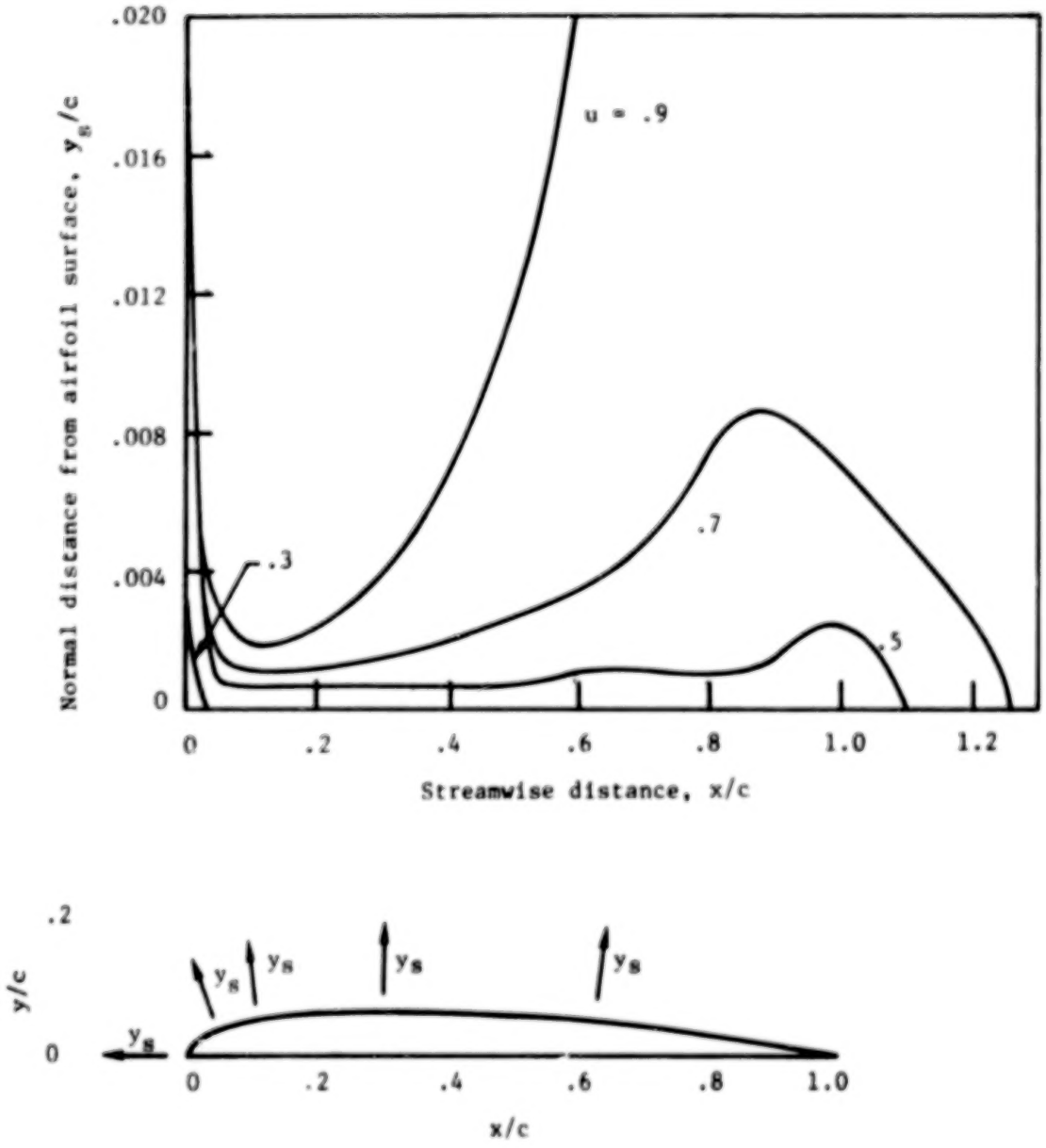

Figure 4. - Isovel contours for NACA 0012 airfoil at zero incidence.

BLANK

PAGE

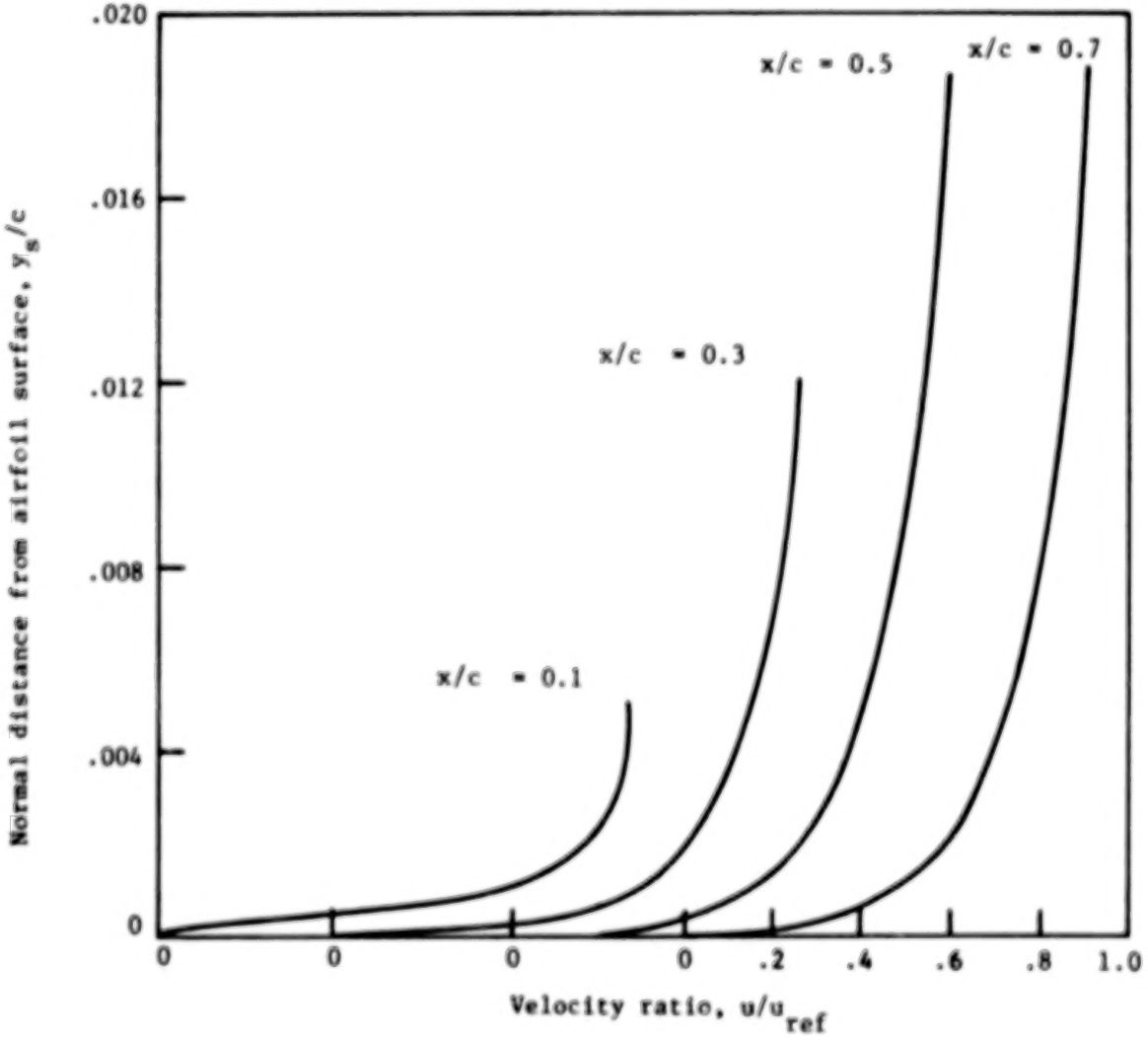

Figure 5. - Velocity profiles for NACA 0012 airfoil at zero incidence.

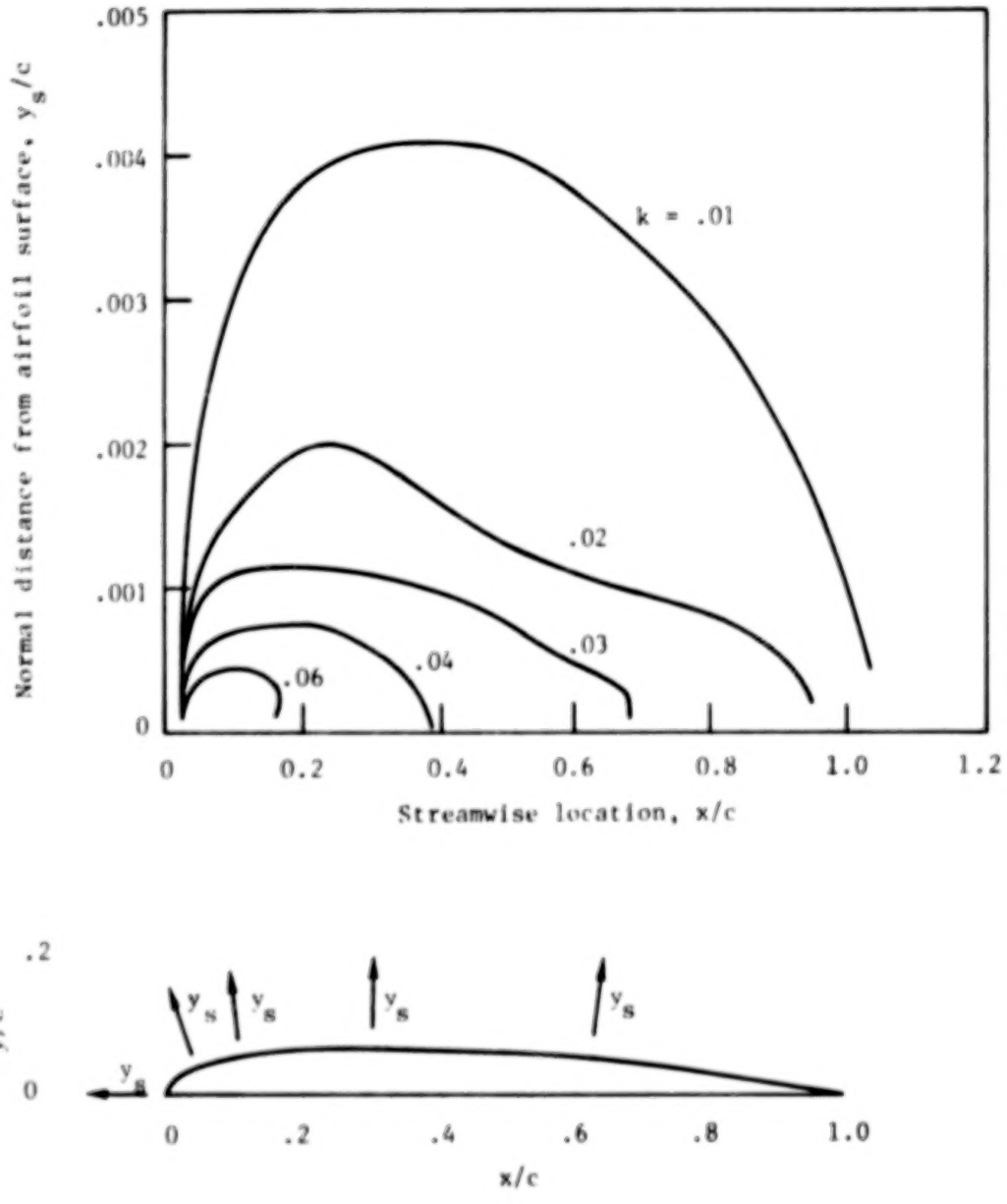

Figure 6. - Turbulence energy isobars for NACA 0012 airfoil at zero incidence.

BLANK

PAGE

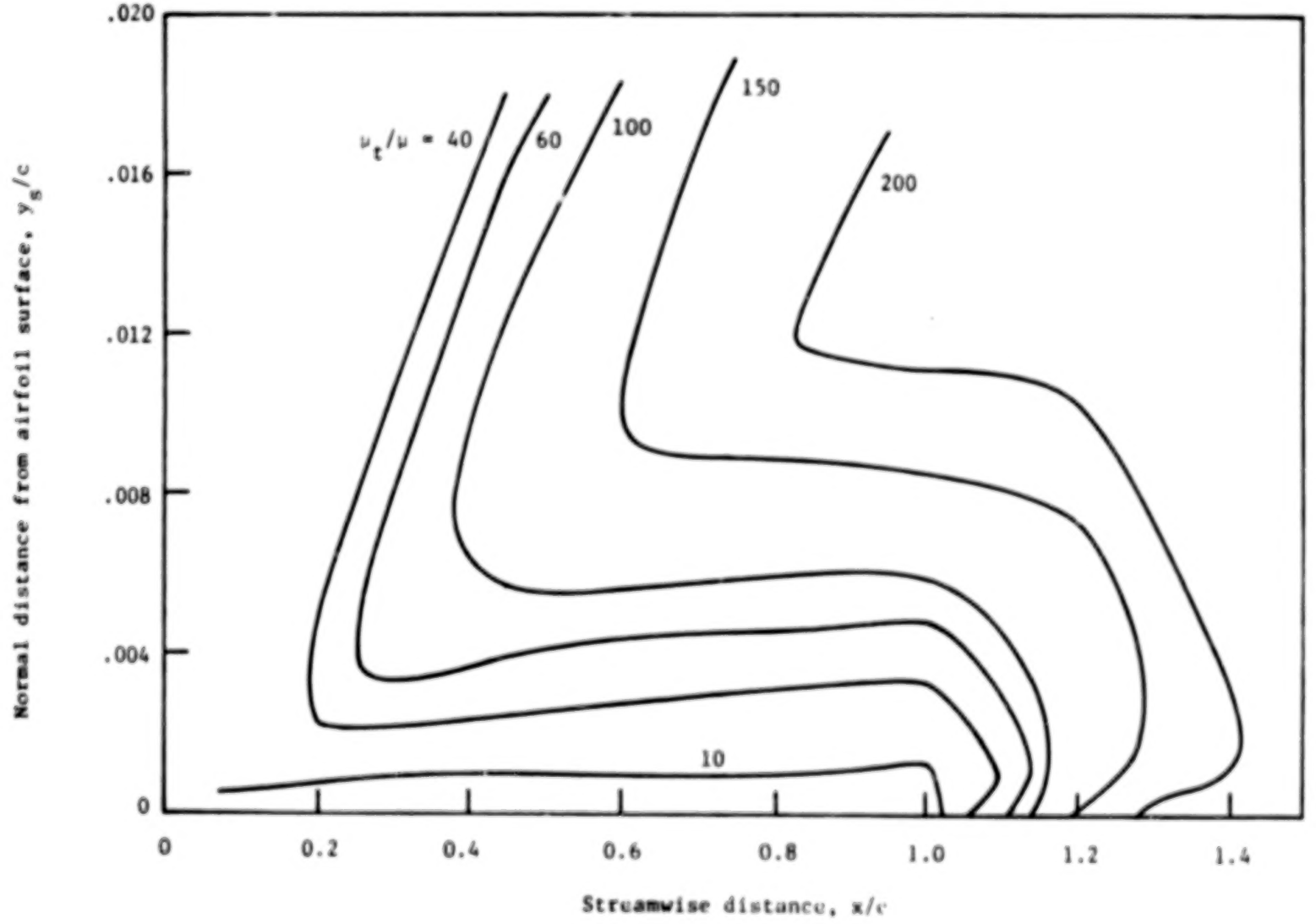

Figure 7. - Viscosity isobars for NACA 0012 airfoil at zero incidence.

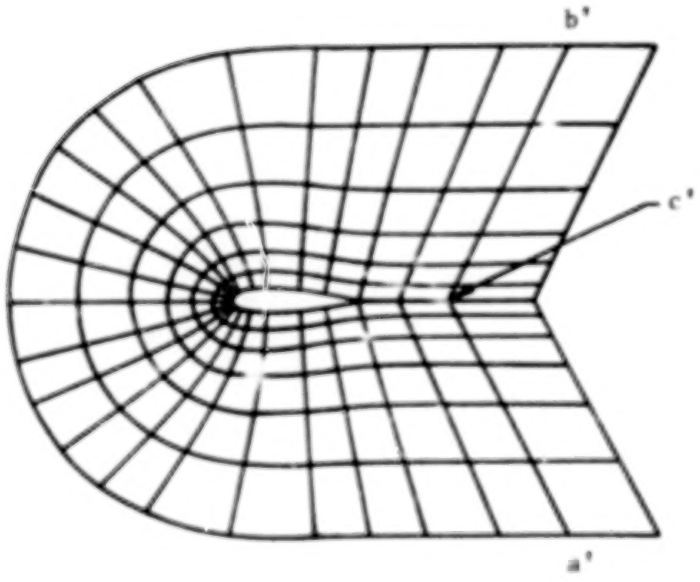

Sketch of Poisson generated coordinate system

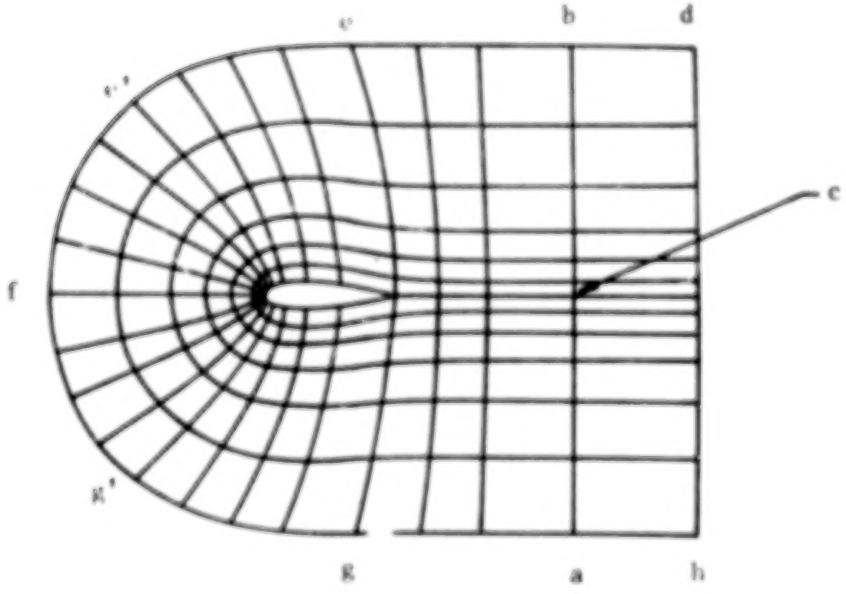

Sketch of constructive coordinate system

Figure 8. - Comparison of coordinate system generated by solution of Poisson equation and constructive coordinate system.

BLANK

PAGE

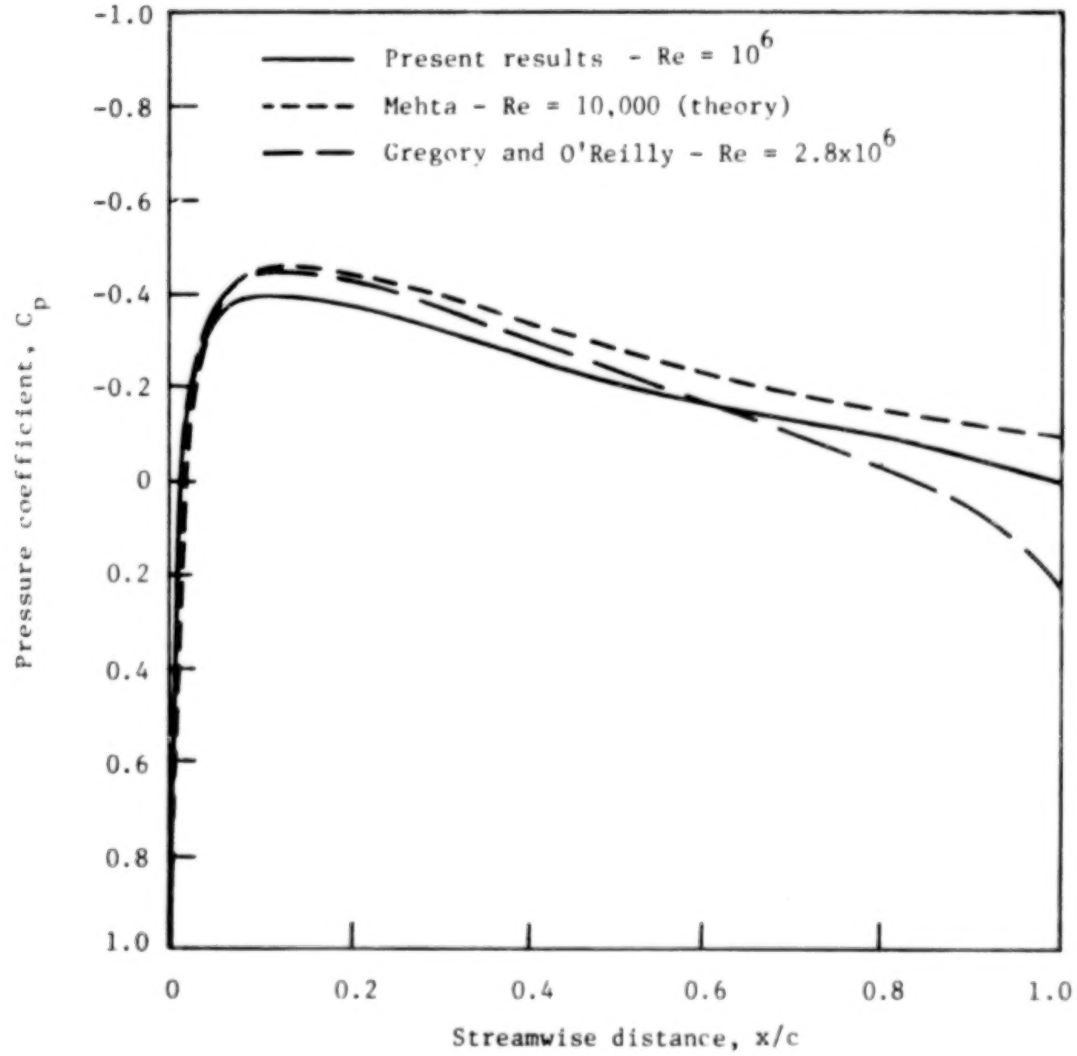

Figure 9. - Surface pressure distribution for NACA 0012 airfoil at zero incidence (full airfoil calculation).

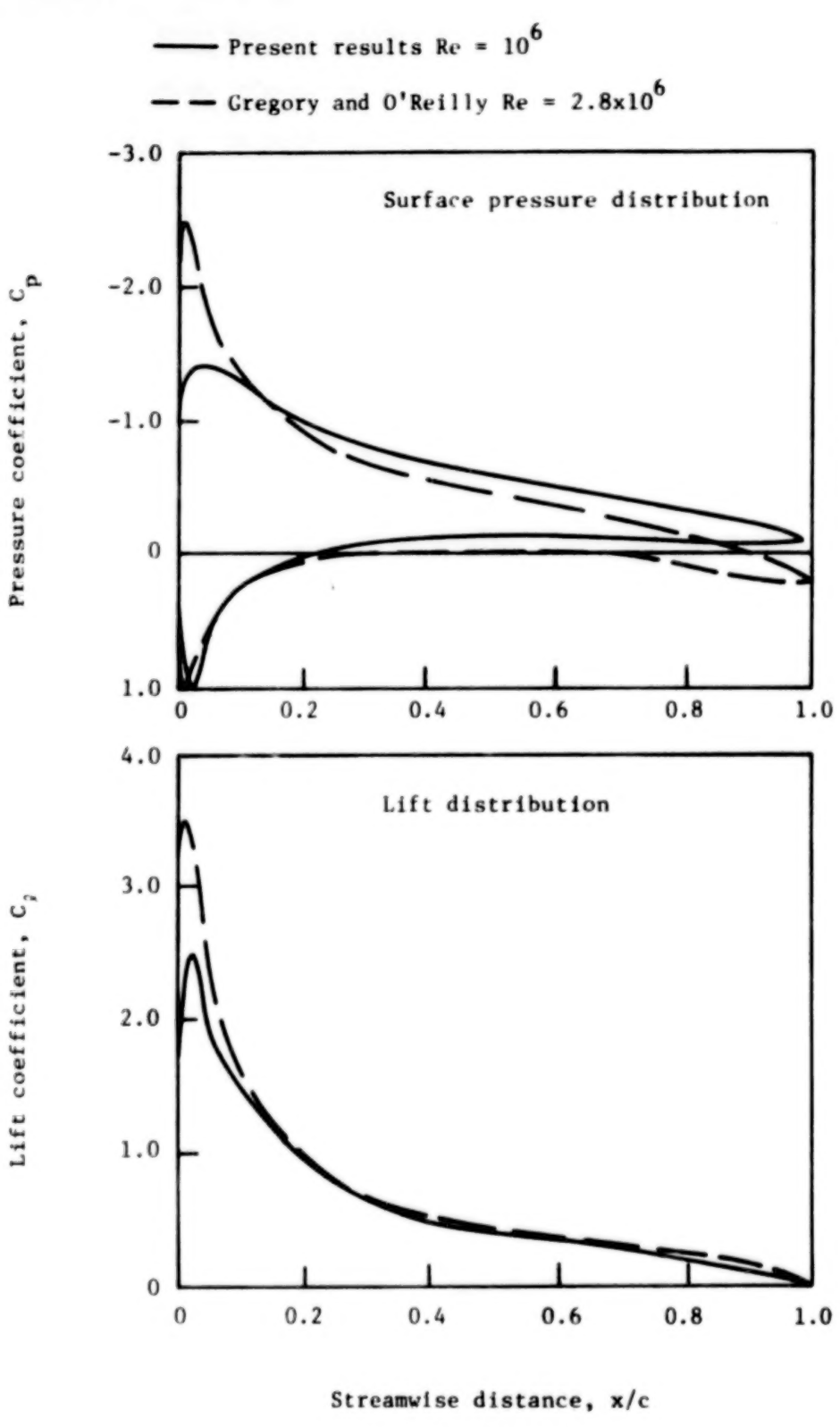

Figure 10. - Surface pressure distribution for NACA 0012 airfoil at 6^o incidence.

BLANK

PAGE

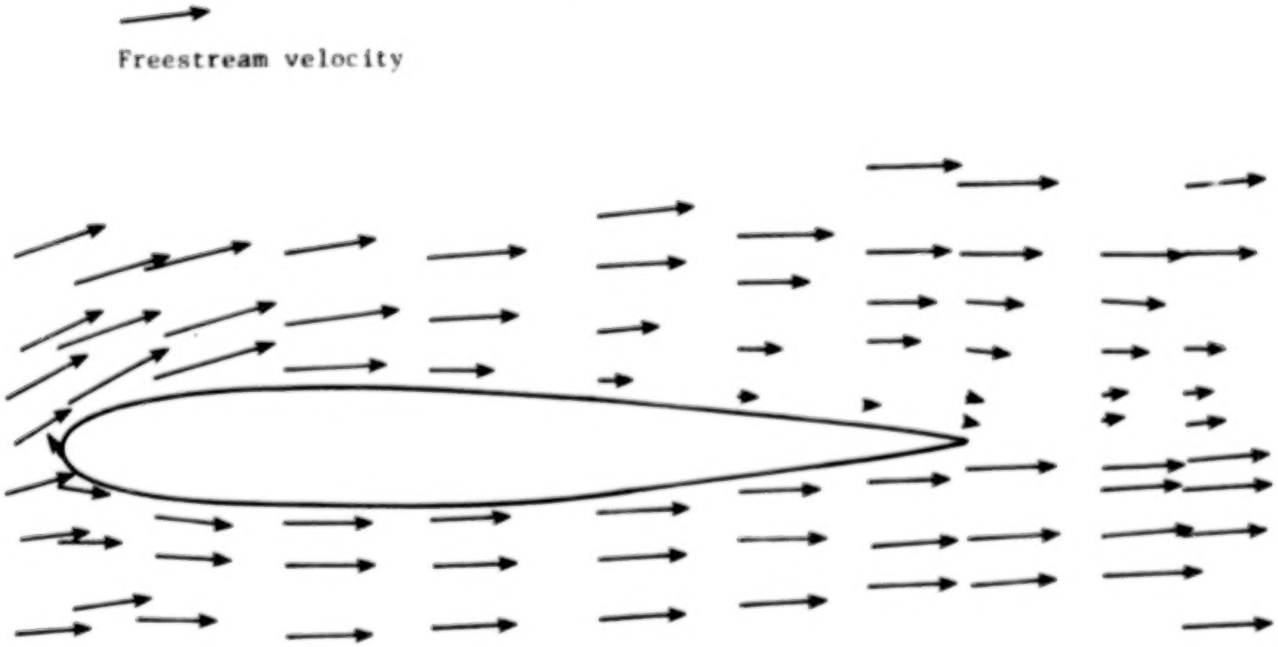

Figure 11. - Velocity field for NACA 0012 airfoil at 6^{o} incidence.

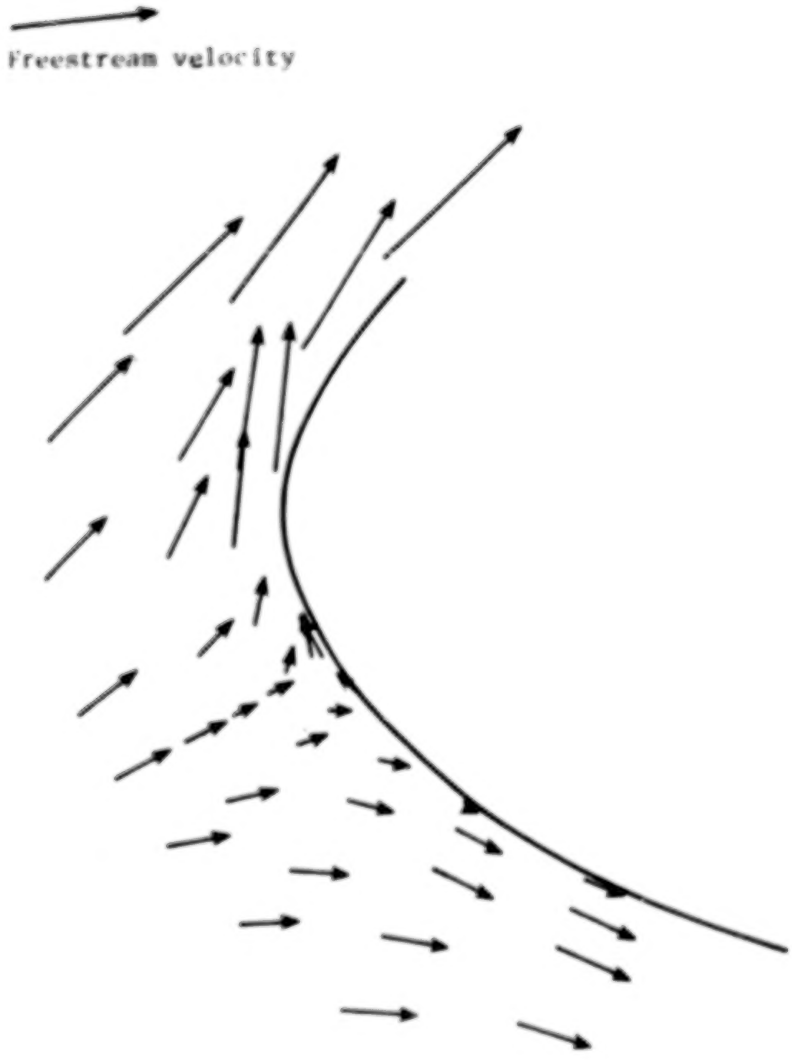

Figure 12. - Velocity field in leading edge region for NACA 0012 airfoil at 6^{0} incidence.

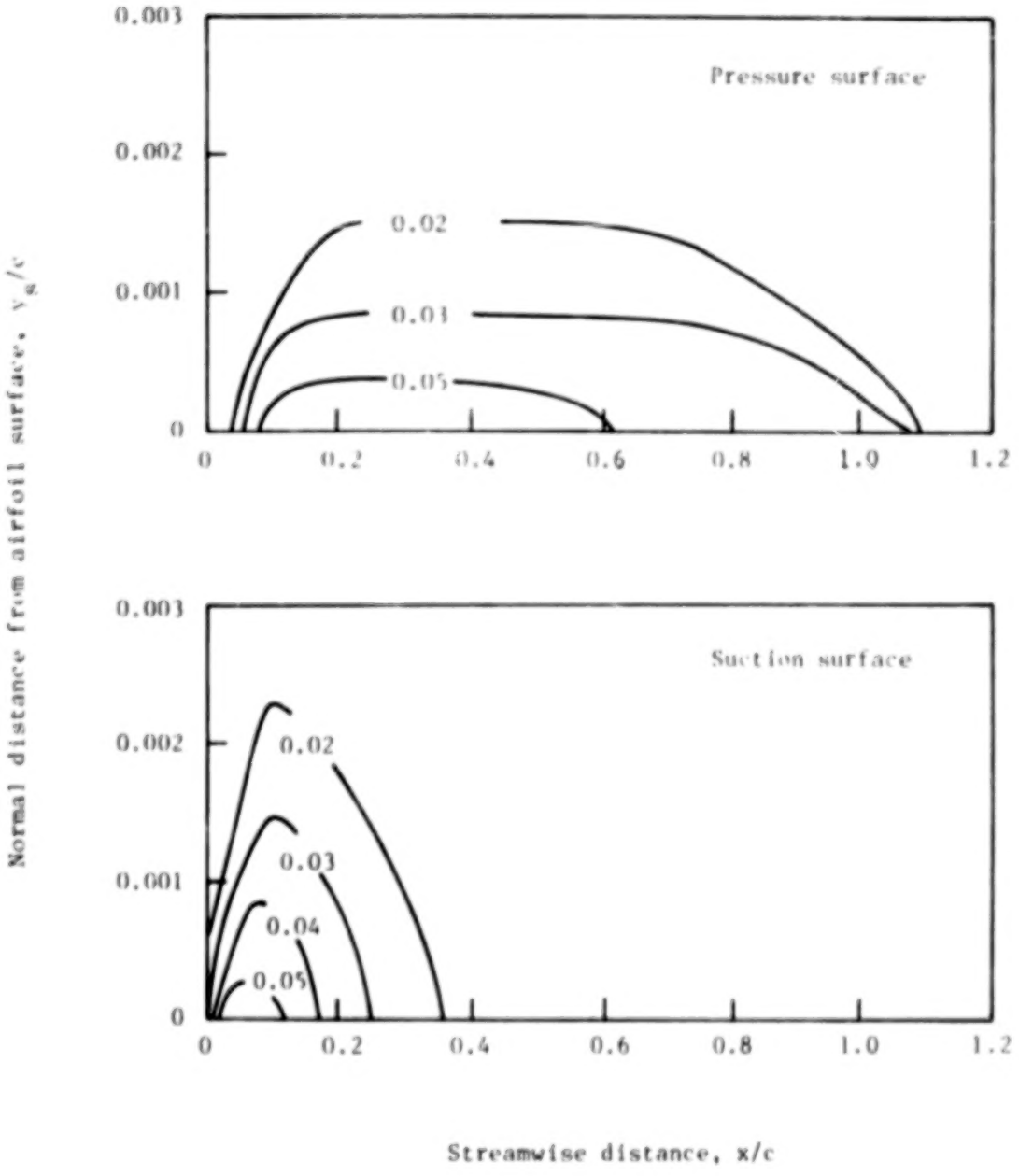

Figure 13. - Turbulence energy contours - NACA 0012 airfoil at 6° incidence.

1. Report No.	2. Government Accession No.	3. Recipient's Catalog No.
NASA CR-3183		

4. Title and Subtitle	5. Report Date
A Compressible Solution of the Navier-Stokes Equations for Turbulent Flow About an Airfoil	October 1979
	6. Performing Organization Code

7. Author(s)	8. Performing Organization Report No.
S. J. Shamroth and H. J. Gibeling	
	10. Work Unit No. 505-10-23-07

9. Performing Organization Name and Address	11. Contract or Grant No.
Scientific Research Associates, Inc. Box 498 Glastonbury, CT 06033	NAS1-15214
	13. Type of Report and Period Covered
12. Sponsoring Agency Name and Address	Contractor Report
National Aeronautics and Space Administration Washington, DC 20546	14. Army Project No.

15. Supplementary Notes

The contract research effort was financially supported by the U.S. Army Research and Technology Laboratories (AVRADCOM), Structures Laboratory.
Langley Technical Monitor: Warren H. Young, Jr. Progress Report

16. Abstract

A compressible time-dependent solution of the Navier-Stokes equations including a transition-turbulence model is obtained for the isolated airfoil flow field problem. The equations are solved by a consistently split linearized block implicit scheme due to Briley and McDonald. A nonorthogonal body-fitted coordinate system is used which has maximum resolution near the airfoil surface and in the region of the airfoil leading edge. The transition-turbulence model is based upon the turbulence kinetic energy equation and predicts regions of laminar, transitional and turbulent flow. Mean flow field and turbulence field results are presented for an NACA 0012 airfoil at zero and nonzero incidence angles at Reynolds number up to one million and low subsonic Mach numbers.

17. Key Words (Suggested by Author(s))	18. Distribution Statement
Navier-Stokes Airfoil stall Dynamic Stall Nonorthogonal grid Turbulent flow	Unclassified - Unlimited Subject Category 02

19. Security Classif. (of this report)	20. Security Classif. (of this page)	21. No. of Pages	22. Price*
Unclassified	Unclassified	65	$5.25

*For sale by the National Technical Information Service, Springfield, Virginia 22161

NASA-Langley, 1979

90%

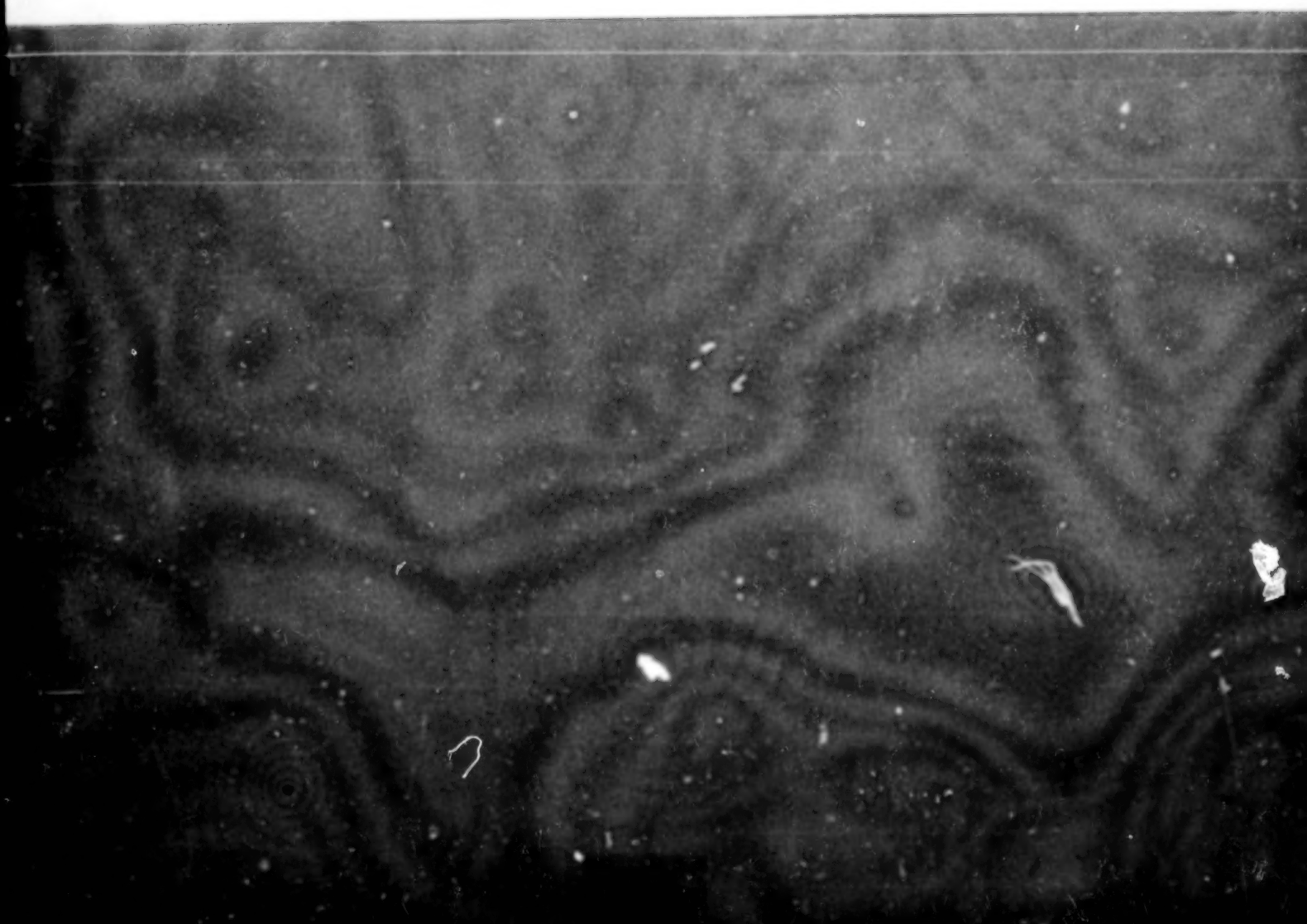

END